

Julia Lyubina

Institute for Metallic Materials,
IFW Dresden, Germany



Characterisation

x-ray diffraction

imaging techniques (SEM, AFM, MFM)

differential scanning calorimetry

Preparation (included in Nanostructured Hard Magnets)

sintering

hydrogen-assisted methods (HD, HDDR)

melt spinning

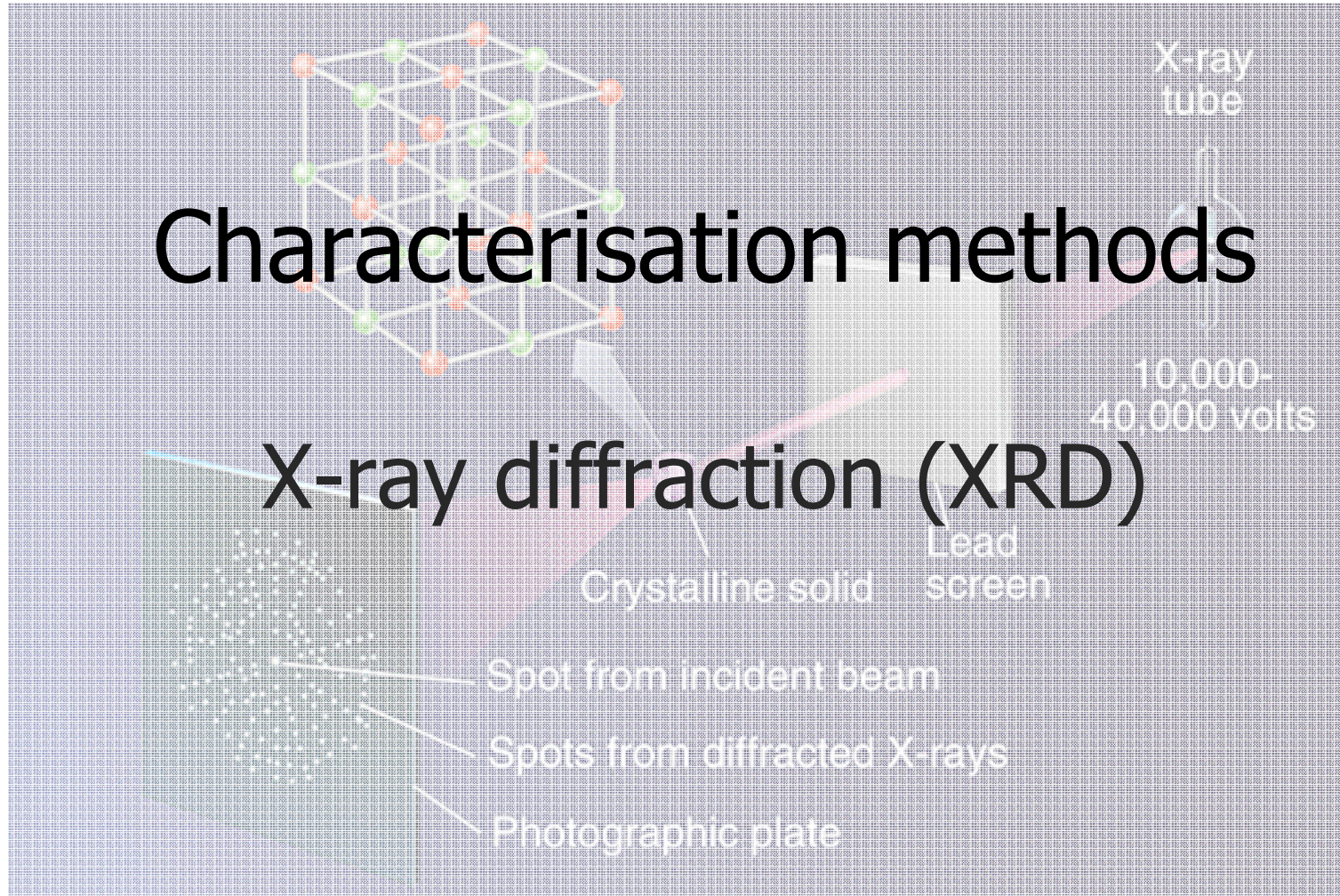
mechanical alloying

hot deformation

Characterisation methods

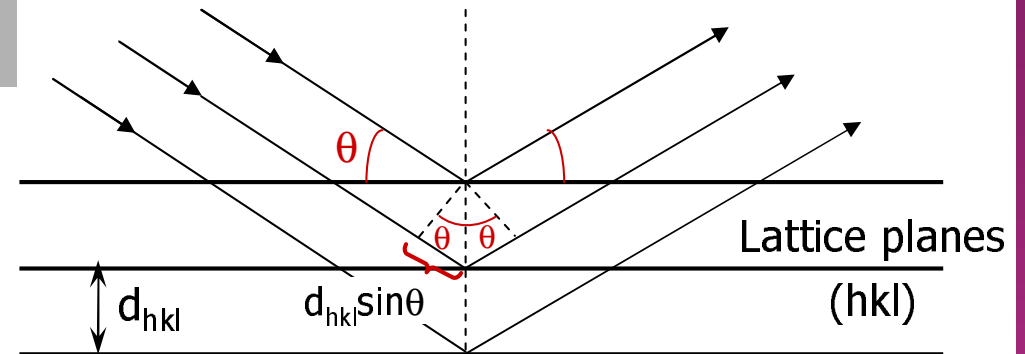
Characterisation methods

X-ray diffraction (XRD)



Bragg's law (elastic scattering)

$$2d_{hkl} \sin \theta = n\lambda$$



Constructive interference \rightarrow
the path length difference = whole number of λ

Properties:

✓ $\sin \theta = 1 \Rightarrow 2d_{hkl} = n\lambda \Rightarrow d_{hkl}^{\min} = \lambda/2$

✓ Diffraction pattern is obtained for

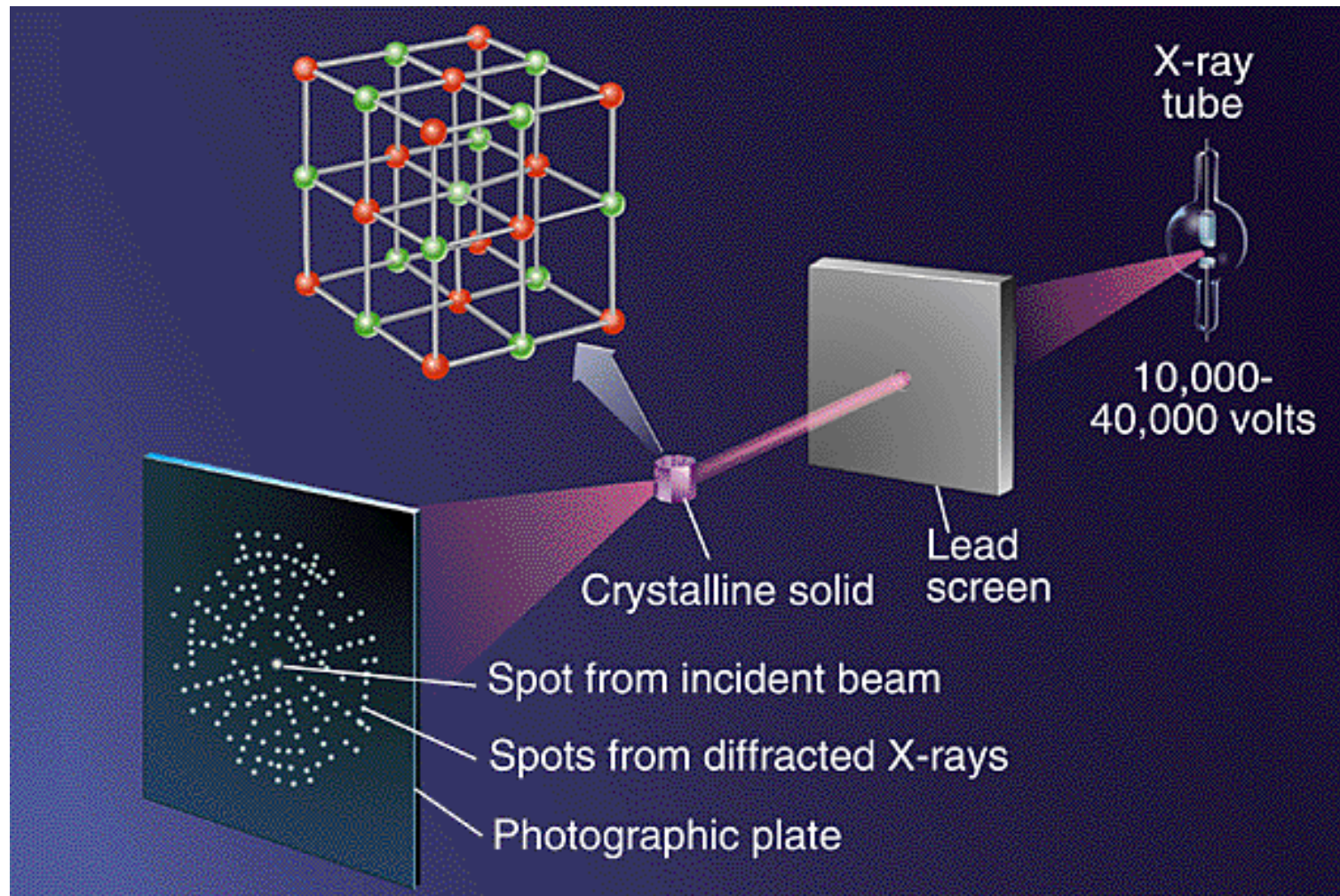
$\theta = \mathbf{var}$, $\lambda = \mathbf{const}$ (powder diffraction, Debye-Scherrer, rotation, Kossel methods)

$\theta = \mathbf{const}$, $\lambda = \mathbf{var}$ (Laue method)

✓ Positions of reflections are determined by the respective set of cell dimensions

X-ray diffraction (XRD)

Diffraction → a crystal placed in an incident beam of hard x-rays reflects this beam in many directions



Structure factor

$$|F_{hkl}|^2 = \left[\sum_{j=1}^N r_j f_j e^{2\pi i(hx_j + ky_j + lz_j)} \right]^2$$

Integrated intensity
(kinematic theory)

$$I_{hkl} = C_0 \cdot |F_{hkl}|^2 \cdot LP \cdot m_{hkl} \cdot e^{-2M} \cdot P_k$$

Kinematic theory:

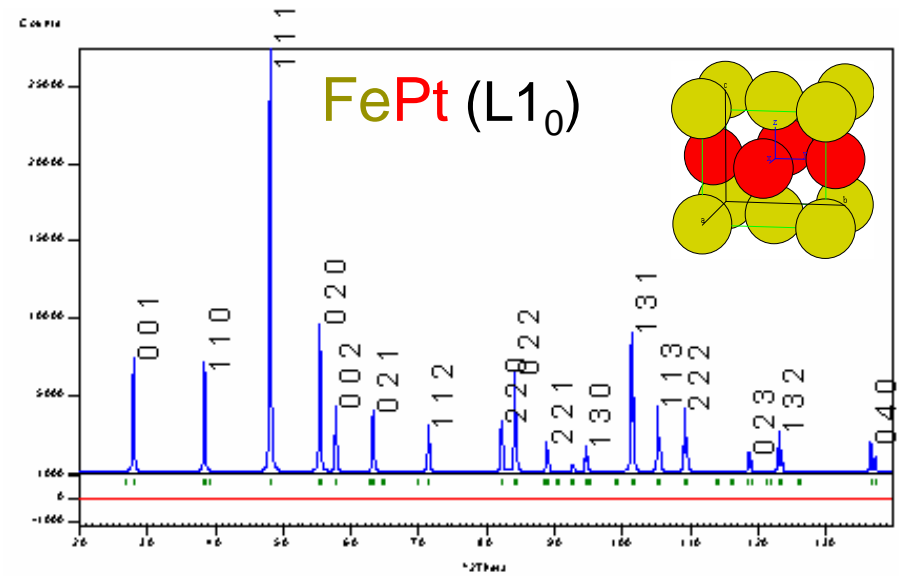
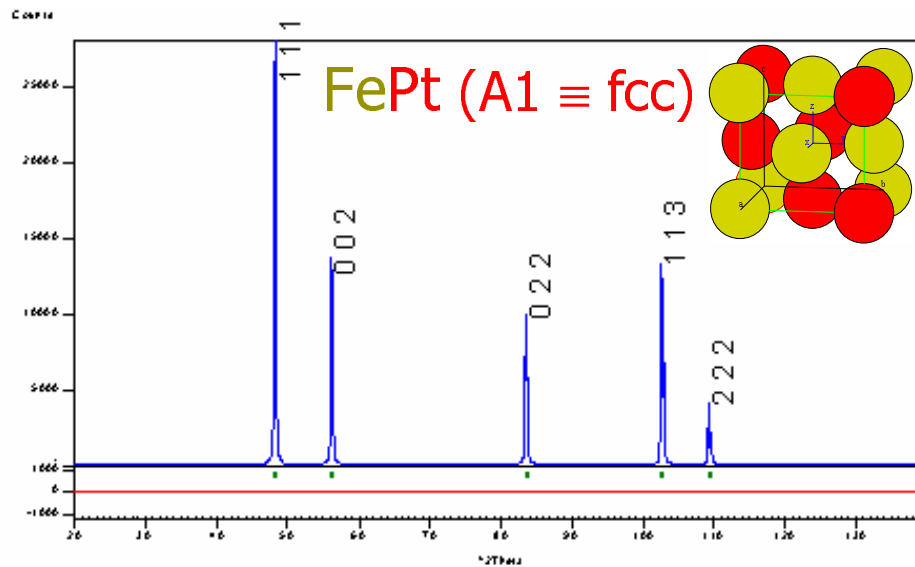
- no interaction between the incident and scattered waves;
- single scattering event;
- no absorption

valid for small crystals ($< 0.5 \mu\text{m}$)
and low scattering power

Dynamic theory:

intensity is weakened due to extinction

Structure factor: chemical ordering



Structure factor

$$|F_{hkl}|^2 = \left[\sum_{j=1}^N r_j f_j e^{2\pi i(hx_j + ky_j + lz_j)} \right]^2$$

Basis

A1 [[000; 1/2 1/2 0; 0 1/2 1/2; 1/2 0 1/2]] **L1₀** [[Pt 000; 1/2 1/2 0; Fe 0 1/2 1/2; 1/2 0 1/2]]

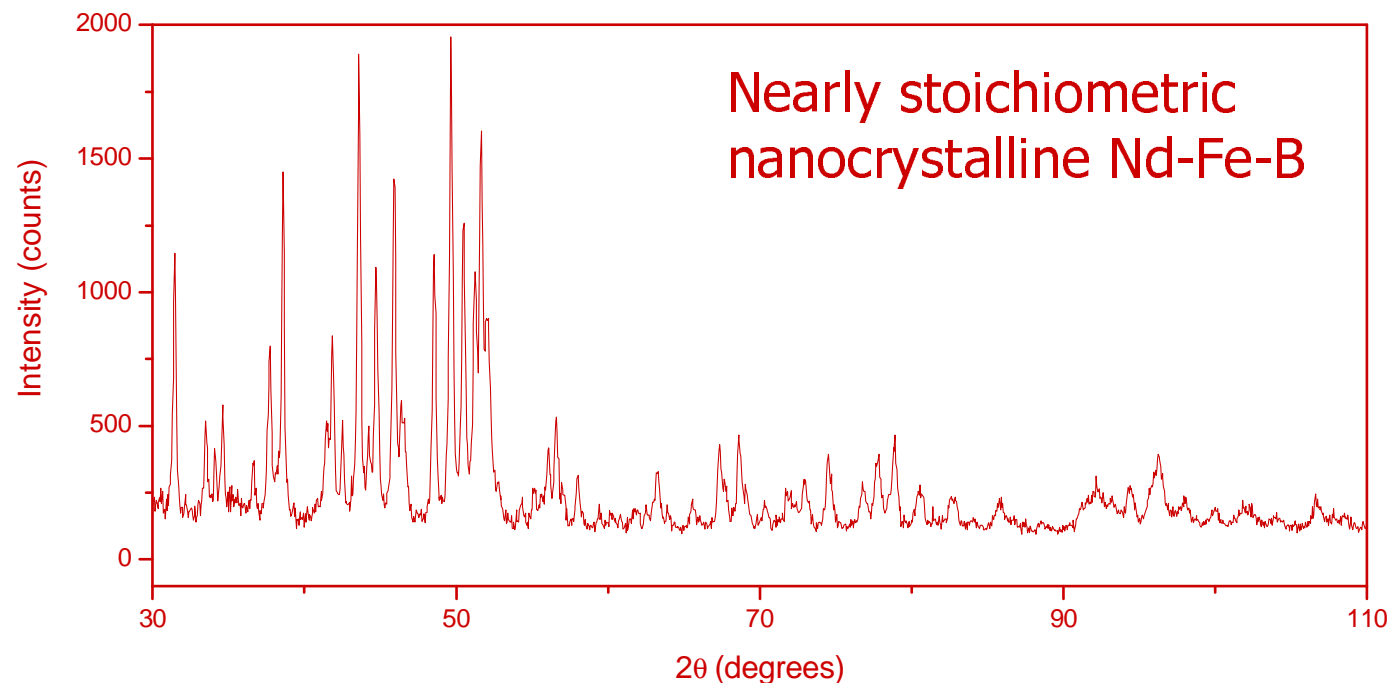
$$F_f = 4(c_{Pt}f_{Pt} + c_{Fe}f_{Fe}) \quad \left. \begin{matrix} hkl \\ \text{even or odd} \end{matrix} \right\} \text{all} \quad \quad F_{ss} = 2S(f_{Pt} - f_{Fe}) \quad \left. \begin{matrix} h+k \\ \text{even} \end{matrix} \right\}$$

The existence of SS reflections is the evidence for ordering!

Qualitative → comparison of the observed data with interplanar spacings d and relative intensities I of known phases

Quantitative → Integrated intensity $I_{hkl} \sim \text{vol. \% of the phase}$

Problem: overlapping diffraction lines!



- ✓ several phases possible
- ✓ low symmetry
- ✓ large cell

Independent determination of peak position and I not possible

Rietveld refinement → a whole-pattern fitting with parameters of a model function depending on the crystallographic structure, instrument features and numerical parameters

Calculated intensity

$$y_{ci} = y_{bi} + \sum_p s_p \sum_k I_{hkl} \phi(2\theta_i - 2\theta_k)$$

↓ background
↓ scale factor ~ vol. %
↓ profile function

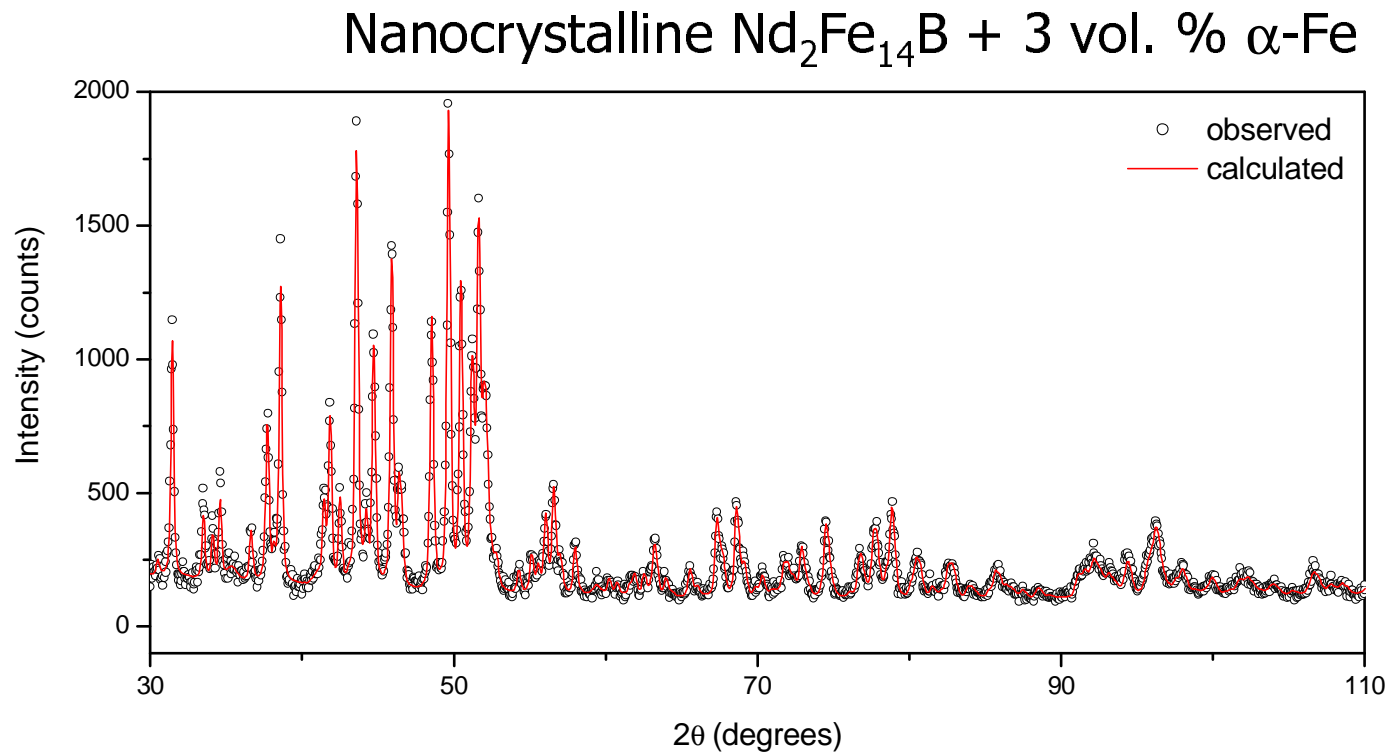
approximates the effects produced by instrument and sample-related features (<D> and <e>)

Aim → find a set of parameters (ξ) describing the observed pattern as good as possible

$$U(\xi) = \sum_i \frac{1}{y_i} (y_i - y_{ci})^2 \quad \frac{\partial U}{\partial \xi} = 0$$

ξ : vol. %, lattice and profile parameters, site occupation, preferred orientation...

Even overlapping peaks contribute information about the structure!

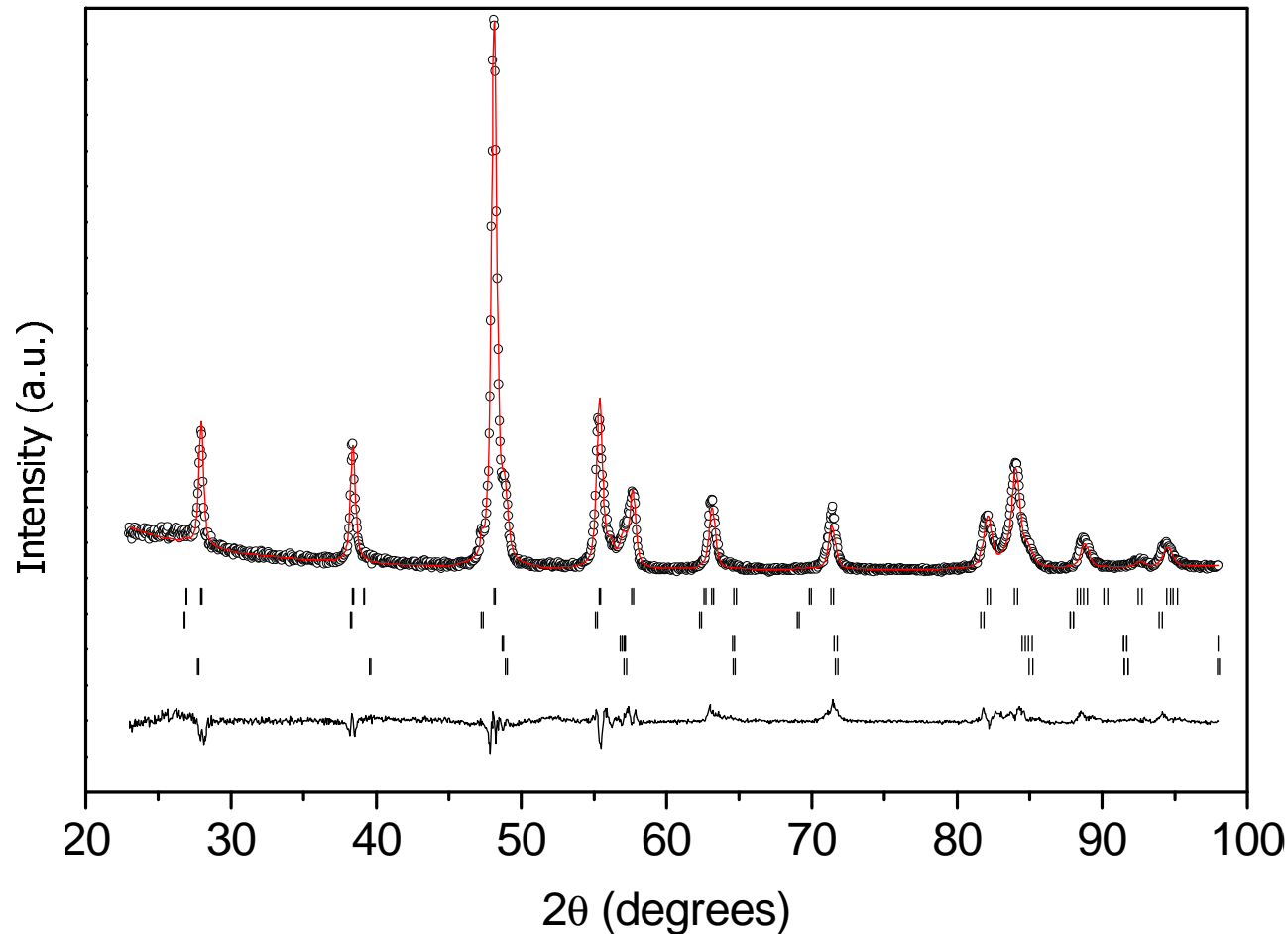


Refined (obtained) parameters

global: background, sample shift

structural: phase fraction, lattice constants, profile parameters (→ grain size/strain)

Phase identification: minority phases



$\text{Fe}_{55}\text{Pt}_{45}$ powder

Qualitative analysis →
 $L1_0$ phase only

Rietveld refinement →
additional phases
A1 FePt, Fe_3Pt and FePt_3

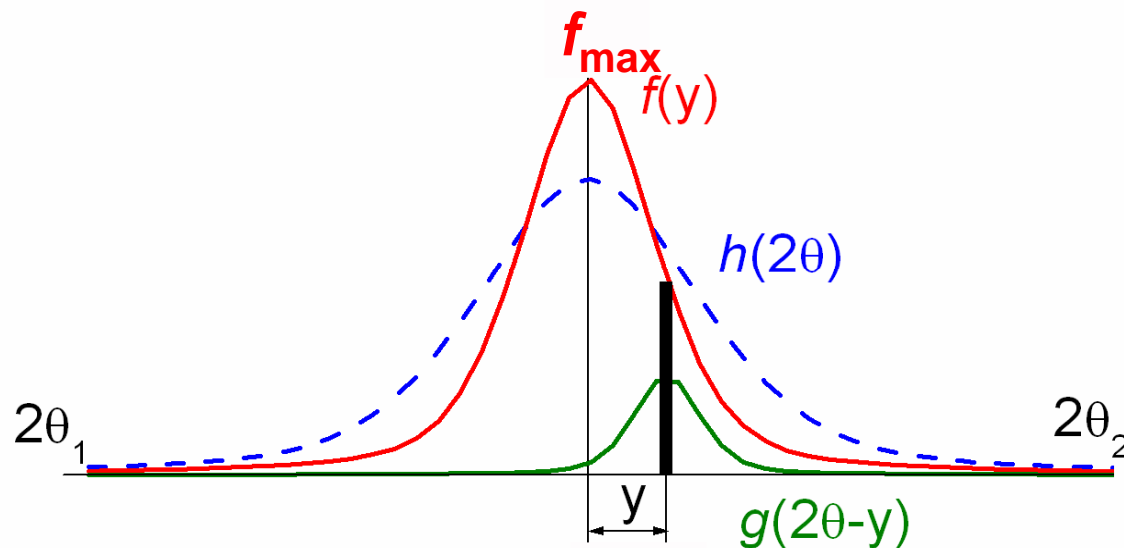
Severe overlap of lines → close cell dimensions

line broadening due to nanocrystallinity

Line broadening: grain size and lattice strain

Observed diffraction profile $h(2\theta)$ is a convolution of the physical $f(2\theta)$ and instrumental $g(2\theta)$ profiles \rightarrow

$$h(2\theta) = \int_{2\theta_1}^{2\theta_2} f(y)g(2\theta - y)dy$$



Integral breadth

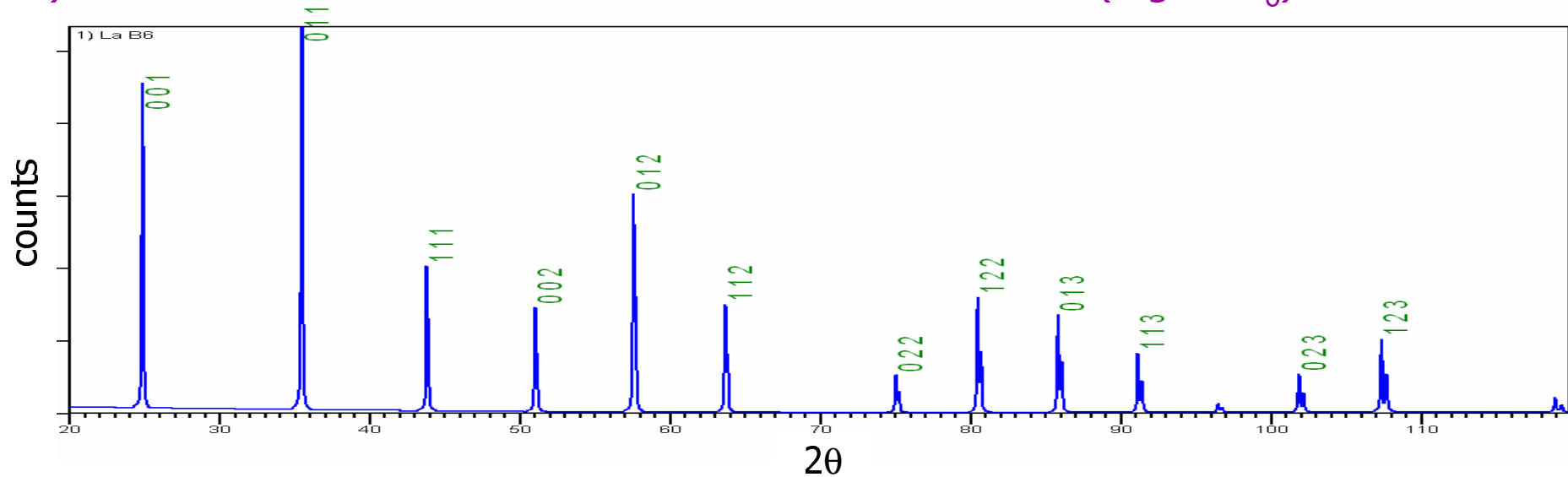
$$\beta = \frac{\int \phi(2\theta)d(2\theta)}{\phi_{\max}}$$

Separate $f(2\theta)$ and $g(2\theta)$ using e.g. integral breadth method

Line broadening: grain size and lattice strain

Separation of $f(2\theta)$ and $g(2\theta)$ using integral breadth method

I) Measurement of a Standard Reference Material SRM (e.g. LaB₆)



II) Select the shape of the peak (e.g. pseudo-Voigt)

IIIa) Interpolate the FWHM of the SRM

$$\Gamma_{IRF}^2 = U \tan^2 \theta + V \tan \theta + W$$

IVa) Correct

$$\Gamma_{sample} = \sqrt{\Gamma_{measured}^2 - \Gamma_{IRF}^2}$$

IIIb) Decompose it into Lorentzian and Gaussian and correct the integral breadths as

$$\beta_L^f = \beta_L^h - \beta_L^g$$

$$(\beta_G^f)^2 = (\beta_G^h)^2 - (\beta_G^g)^2$$

„Average size-strain“ method

/modified Williamson-Hall analysis/

Integral breadths in the reciprocal units

$$\beta^* = \beta \cos \theta / \lambda$$

Lorenzian

Gaussian

$$V = \gamma \frac{\sqrt{4}}{\beta \pi} \left[1 + 4 \left(\frac{2\theta_i - 2\theta_k}{\beta} \right)^2 \right]^{-1} + (1 - \gamma) \frac{\sqrt{4 \ln 2}}{\beta \sqrt{\pi}} \exp \left[-4 \ln 2 \left(\frac{2\theta_i - 2\theta_k}{\beta} \right)^2 \right]$$

size effects

$$\beta_L^* = 1 / \varepsilon$$

strain effects

$$\beta_G^* = \eta d^* / 2$$

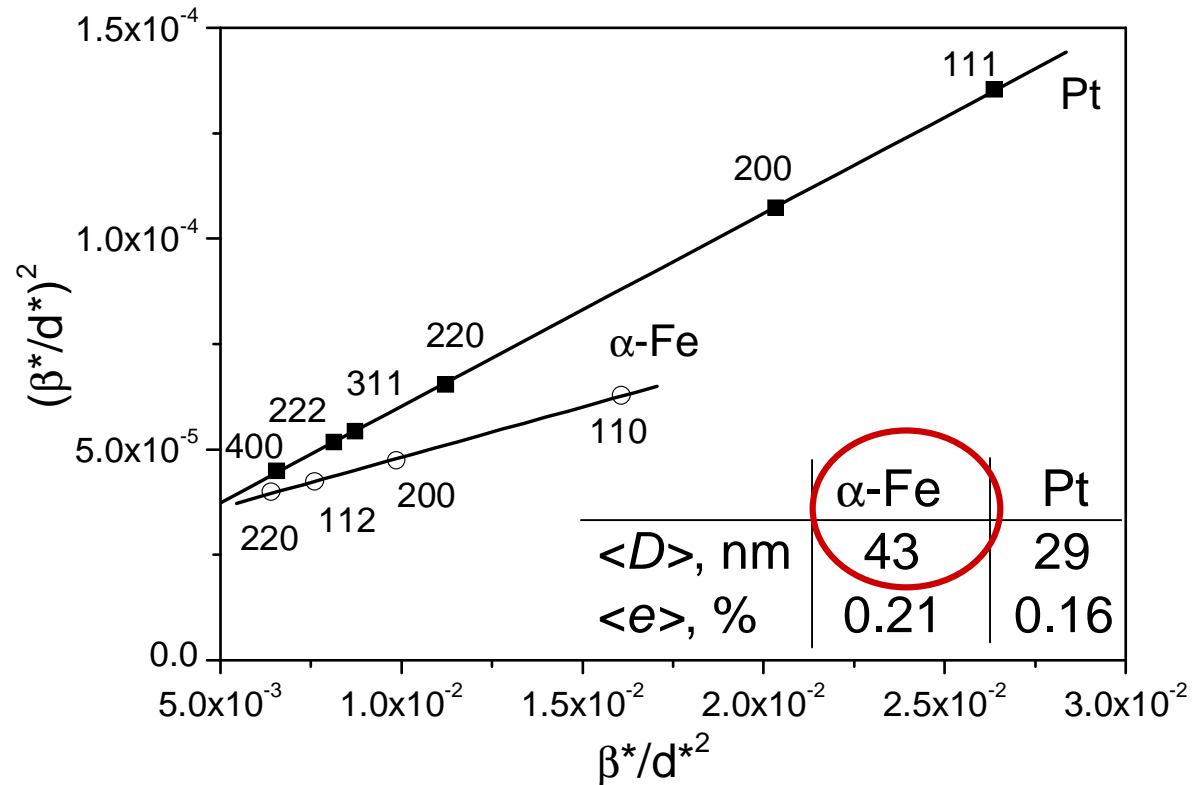
$$\beta^2 = \beta_L \beta + \beta_G^2 \Rightarrow (\beta^* / d^*)^2 = \varepsilon^{-1} \beta^* / (d^*)^2 + (\eta / 2)^2$$

„Average size-strain“ method

$$(\beta^* / d^*)^2 = \varepsilon^{-1} \beta^* / (d^*)^2 + (\eta / 2)^2$$

Spherical particle
 $\langle D \rangle = 1.333\varepsilon$

rms strain
 $\langle e \rangle = \eta / 2\sqrt{2\pi}$



Scherrer eq.:

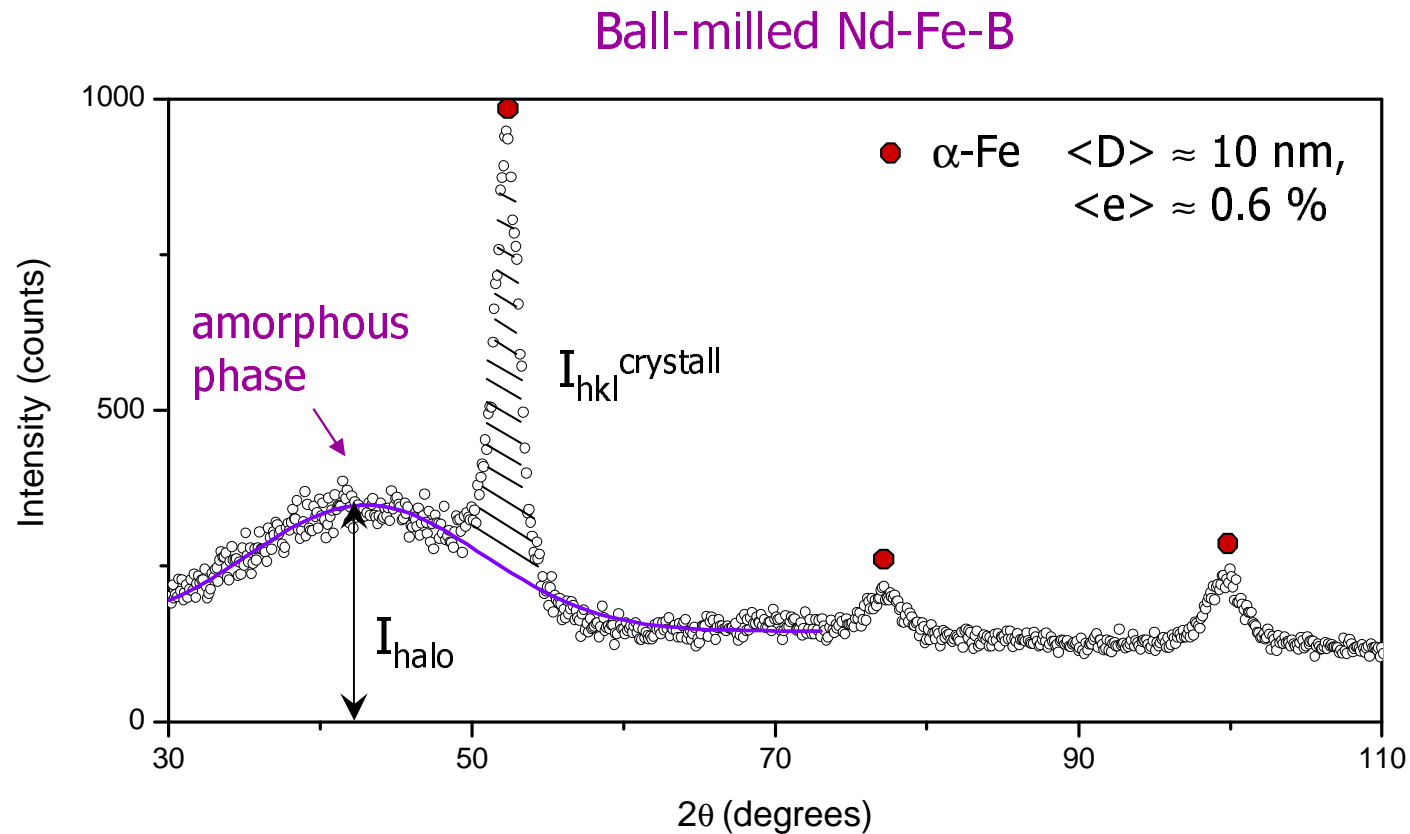
$$\langle D \rangle = 0.9\lambda / \beta \cos \theta$$

\Rightarrow for α -Fe $\langle D \rangle = 15$ nm!

$\langle D \rangle_{\text{XRD}} \approx 5 \dots 200$ nm

Diffraction from amorphous materials

Amorphous materials → the atoms has permanent neighbours, but there is no repeating structure (short range order).

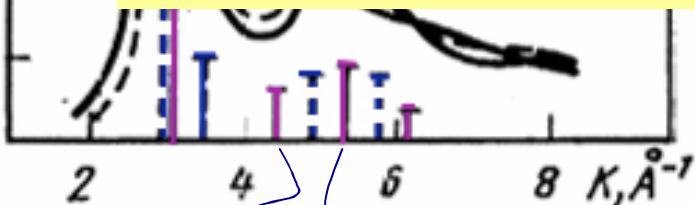
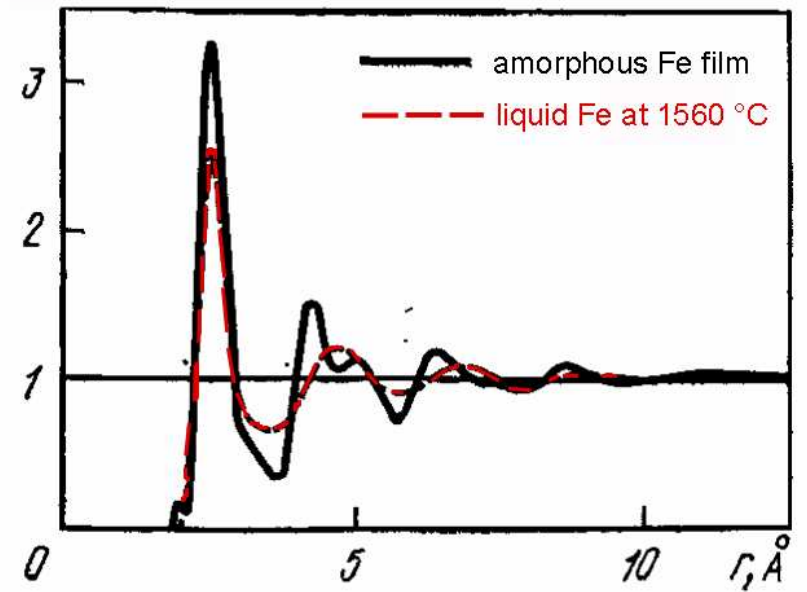
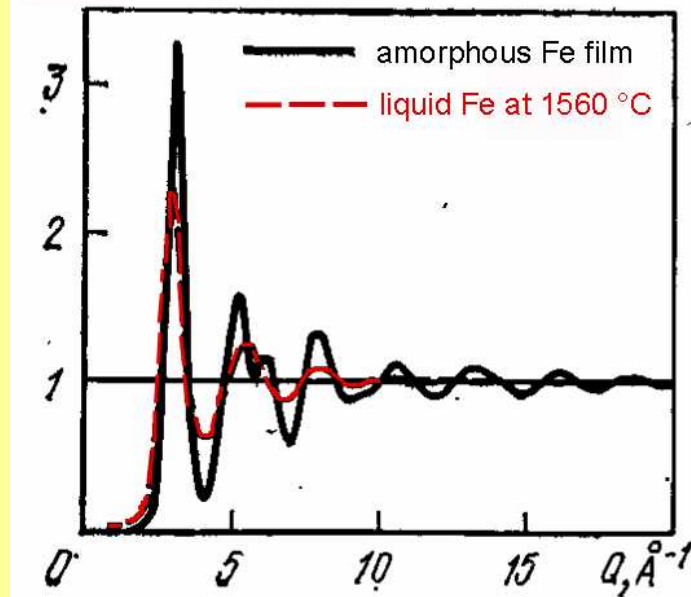
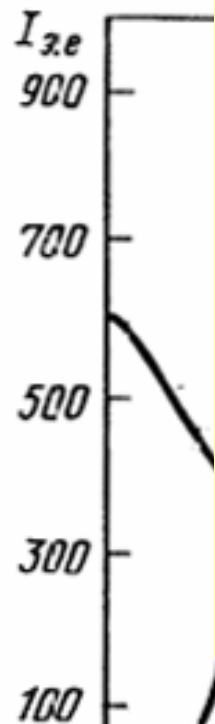


Diffraction from amorphous materials

S
(struc

Scattering intensity I
(structure factor)

Radial distribution function
 $4\pi R^2\rho(R)$



bcc

fcc

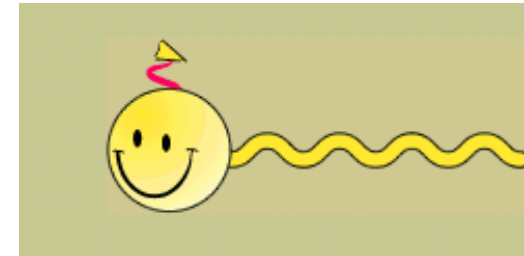
Radial distribution function

$$4\pi R^2\rho(R)$$

radial function of atomic density

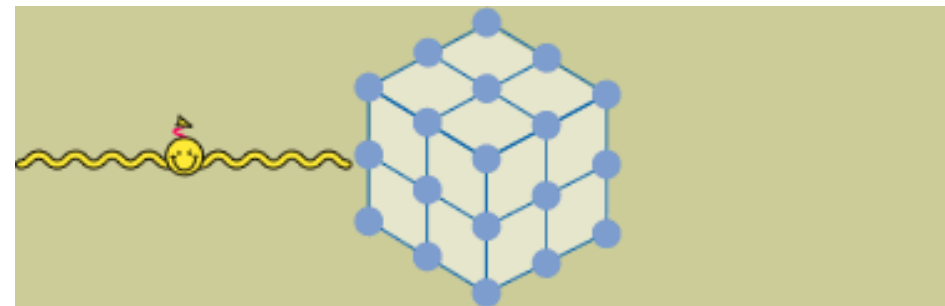
coord. sphere
radius

- Behave either as particles or as waves
- Wavelength varies depending on the source temp.:
hot (0.2-1 Å), thermal (1-4 Å), cold (3-30 Å)



Nuclear scattering

interaction with the nucleus via strong nuclear force → crystal structure determination from diffraction experiments



Magnetic scattering

The neutron possesses a spin → can be scattered from variations in magnetic field via the electromagnetic interaction → magn. structure probe

Structure factor

$$|F_{hkl}|^2 = \left[\sum_{j=1}^N f_j e^{2\pi i(hx_j + ky_j + lz_j)} \right]^2 \sim I_{\text{int}}$$

X-rays

f_j - atomic form factor

X-rays interact with e^- cloud

$$\Rightarrow f_j \sim Z$$

Neutrons

$f_j(b_j)$ - neutron coherent scattering length

Neutrons interact with the nucleus \Rightarrow

$$b_j = \nabla$$

- ↳ Weak absorption \Rightarrow large penetration depth
- ↳ Possibility to locate light atoms or distinguish neighbouring atoms in the periodic table
- ↳ Magnetic structure probe

Example: $L1_0$ FePt

$$Z_{\text{Pt}} (= 78) \gg Z_{\text{Fe}} (= 26)$$

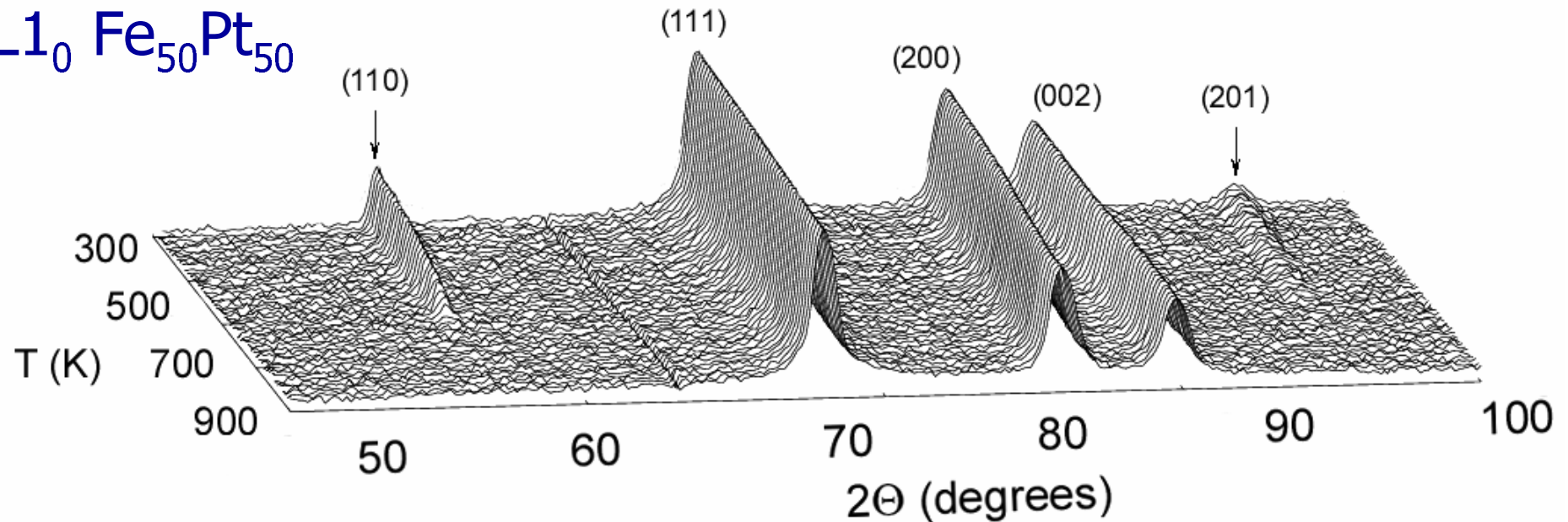
$$\Rightarrow f_{\text{Pt}} \gg f_{\text{Fe}} \text{ BUT } b_{\text{Pt}} \approx b_{\text{Fe}}$$

$$F_{ss} = 2\mathbf{S}(f_{\text{Pt}} - f_{\text{Fe}}) \quad \left. \begin{matrix} h+k \\ \end{matrix} \right\} \text{even}$$

Site occupation (and order parameter \mathbf{S}) determination is possible with x-rays, not with neutrons

Magnetic structure by neutron diffraction

$L1_0$ $Fe_{50}Pt_{50}$

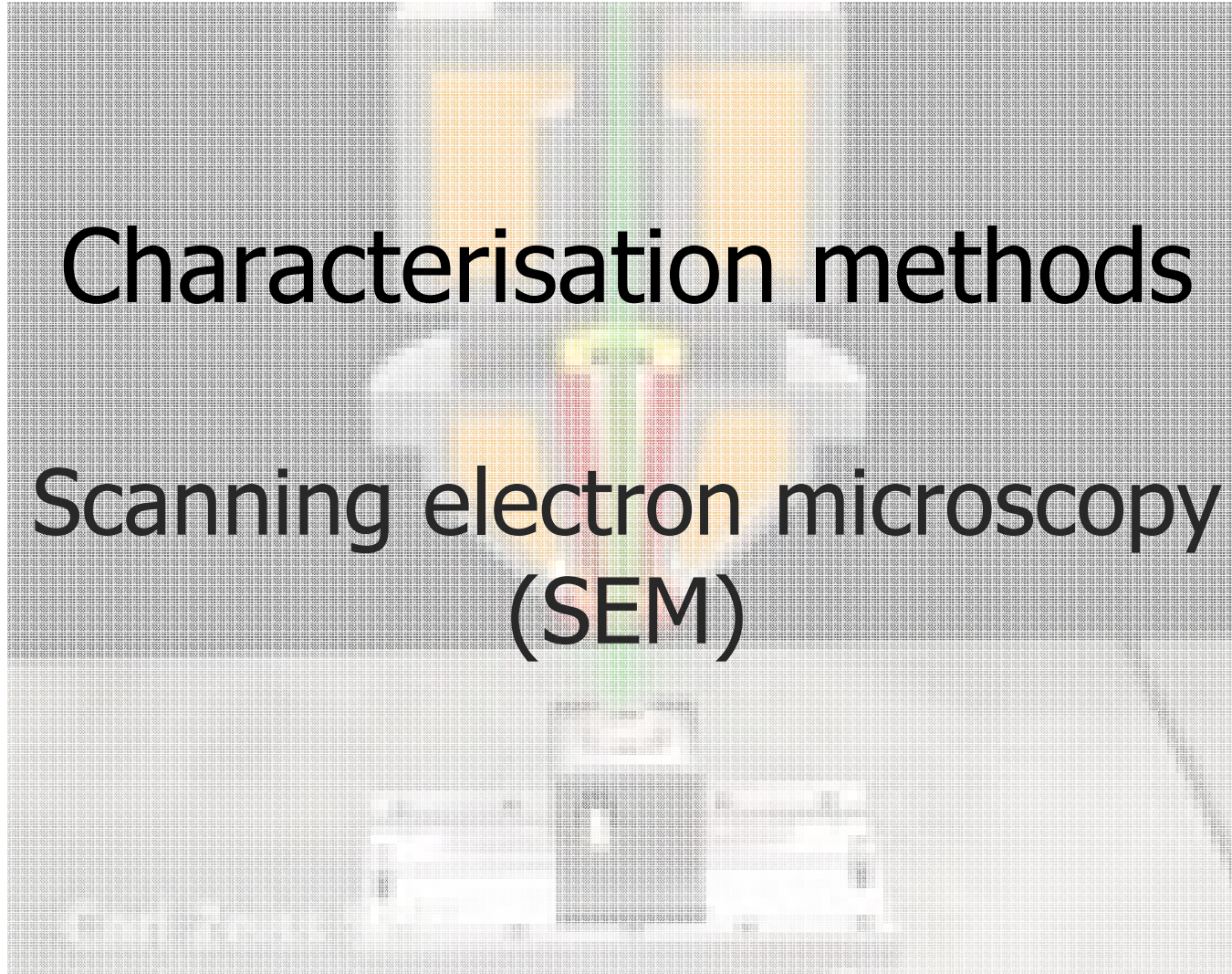


Neutron coherent scattering length $b_{Pt} \approx b_{Fe}$

- Magnetic reflections evolve on cooling around 725 K
- Int. intensity \sim (magnetic structure factor) $^2 \sim$ (projection of $\mathbf{m} \perp \mathbf{k}$) 2

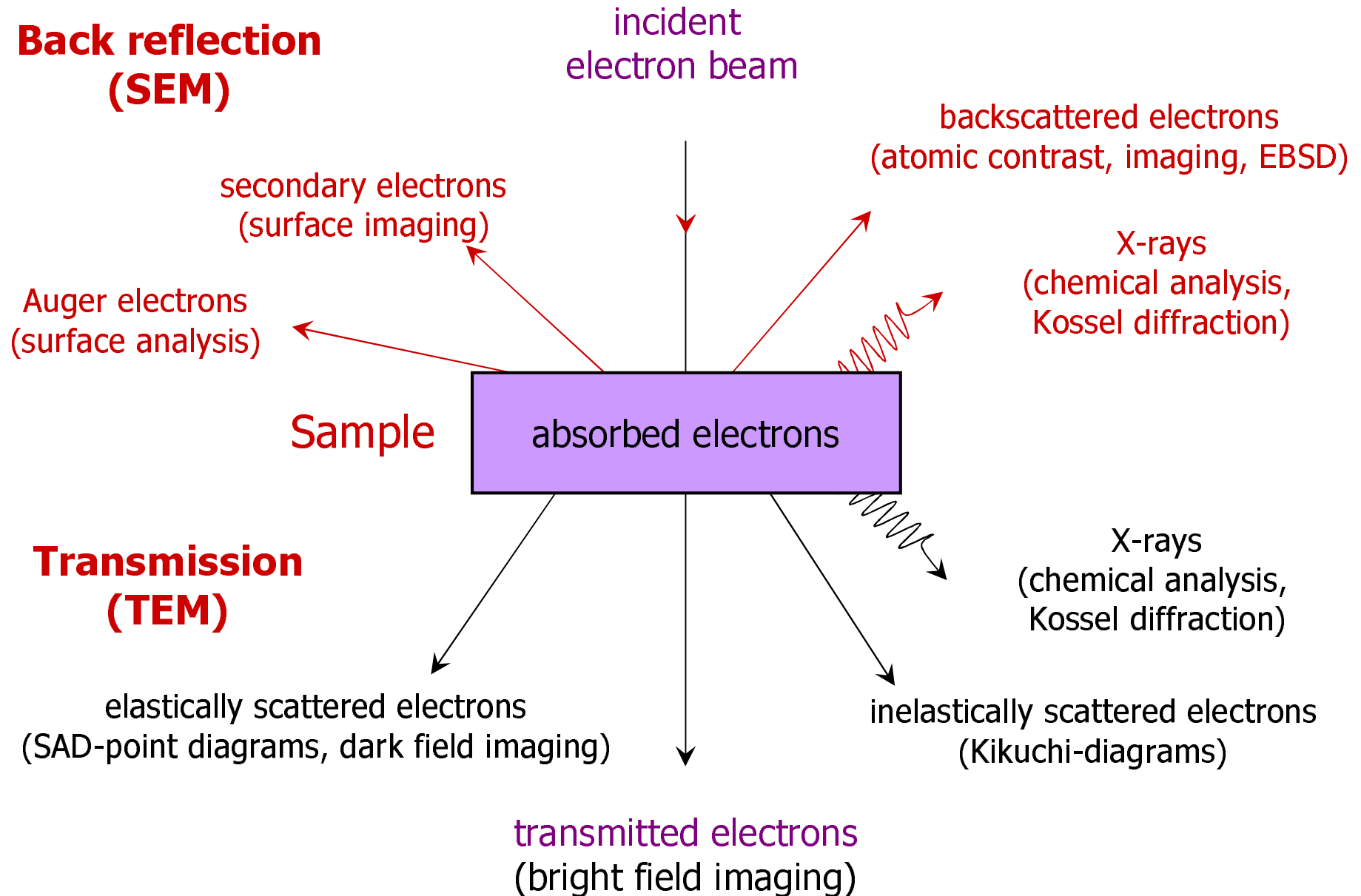
Characterisation methods

Scanning electron microscopy (SEM)

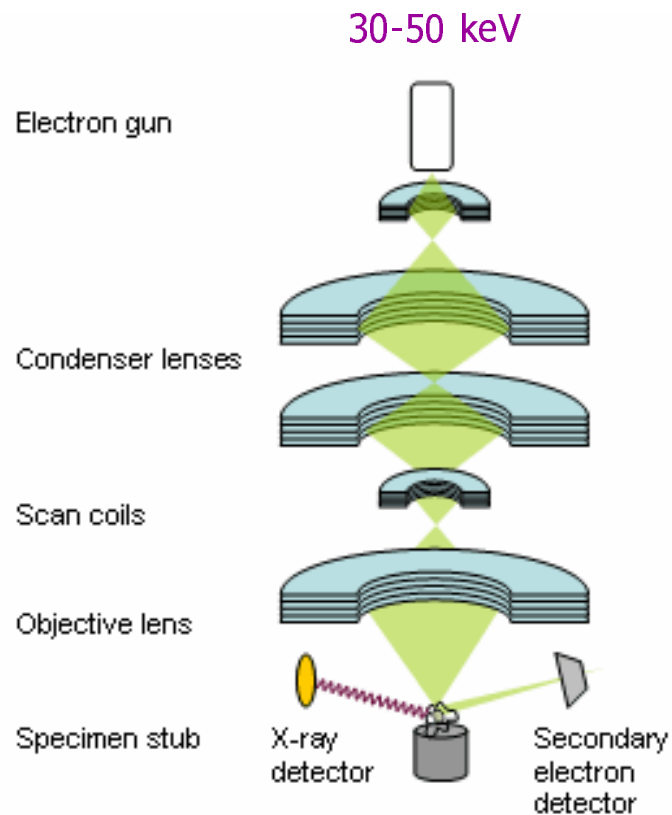


Electron microscopy: interaction of e^- with matter

Back reflection (SEM)



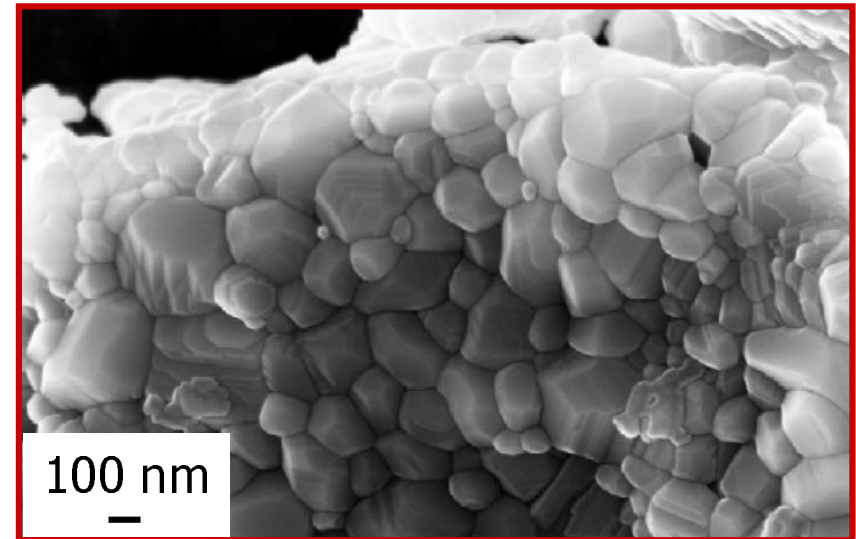
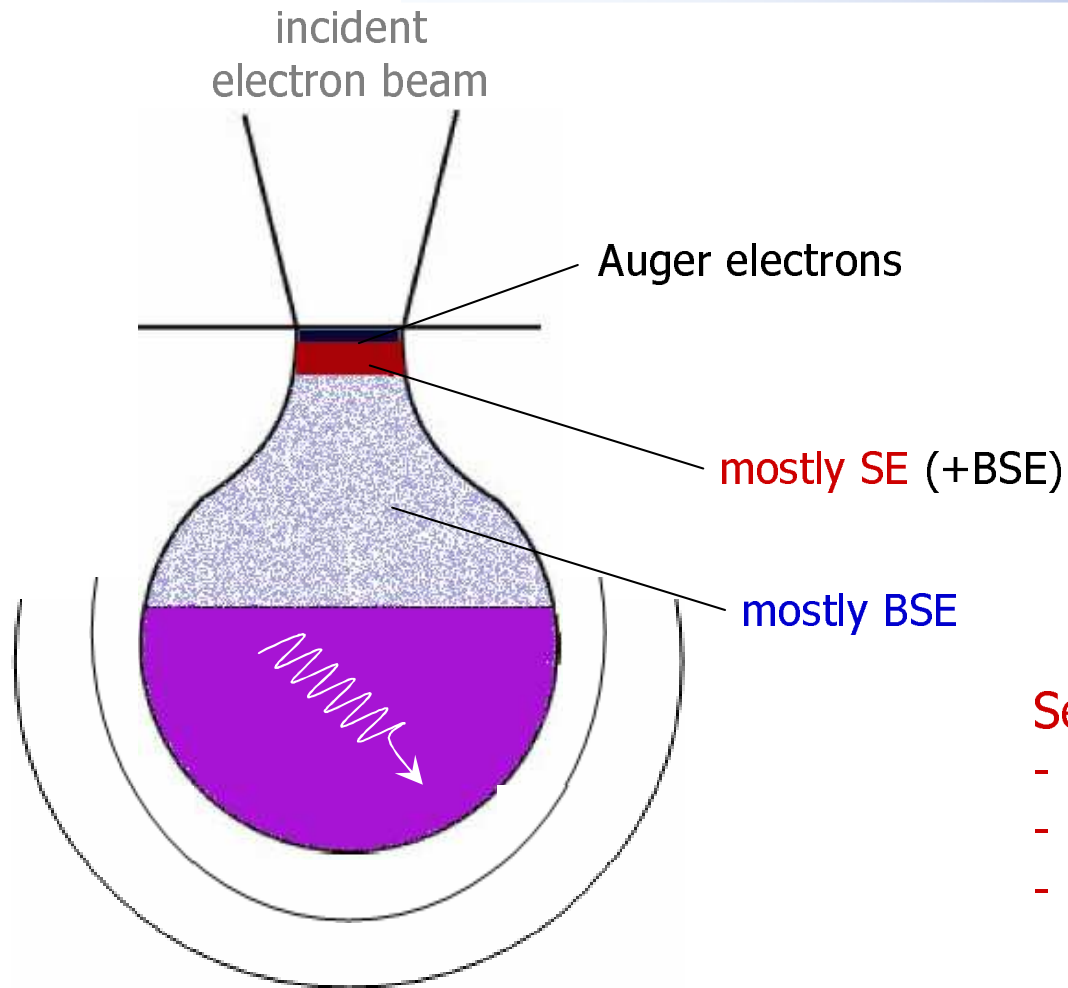
Microscope scheme



Interaction of e⁻ beam with matter in SEM



Scanning electron microscopy (SEM)



Sr-Fe-O, courtesy of K. Khlopkov

Secondary electrons (SE)

- low energy (~ 10 eV)
- surface topographical image
- production is mostly independent of z

Backscattered electrons (BSE)

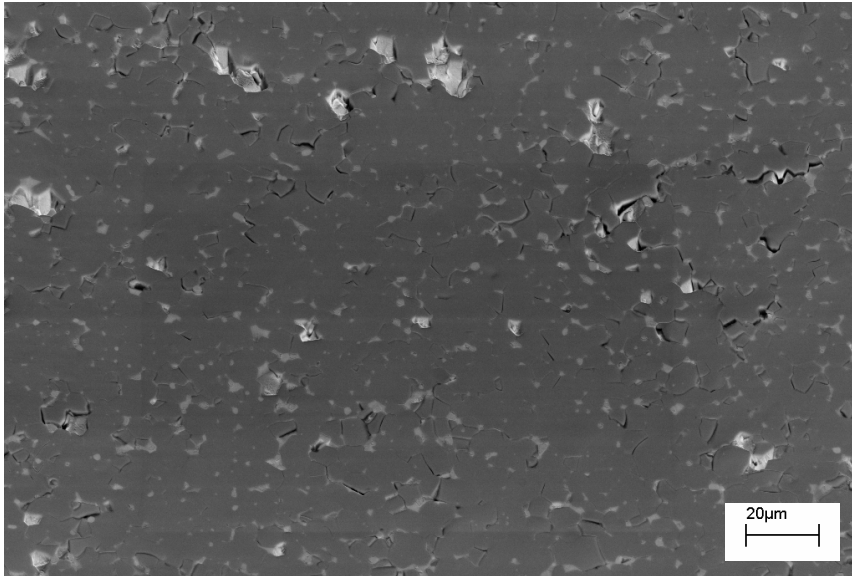
- high energy (> 50 eV)
- large width of escape depth
- heavy elements produce more BSE
 \Rightarrow atomic number contrast

Resolution depends on spot size.

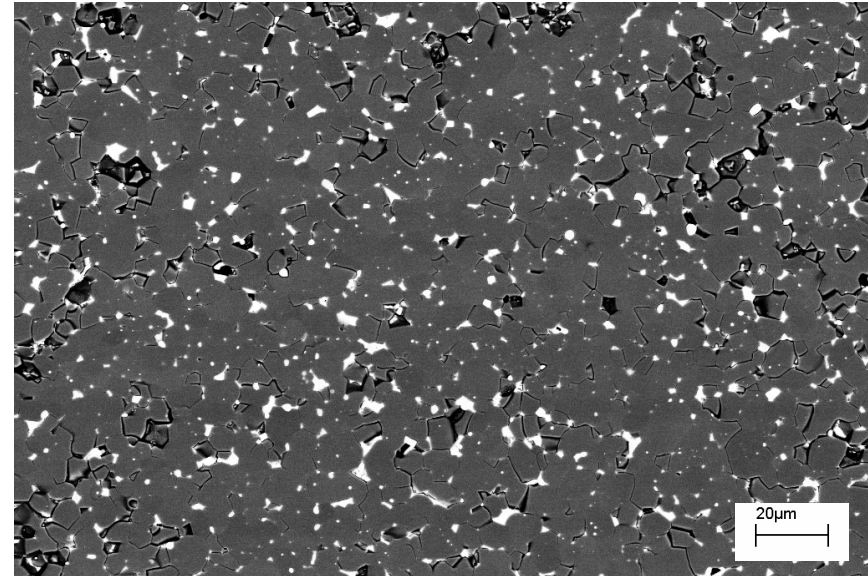
Resolution in SE better than in BSE

\sim several nanometers!

Secondary electrons (SE)



Backscattered electrons (BSE)



Sintered Nd-Fe-B magnet, courtesy of K. Khlopkov

Surface topography image

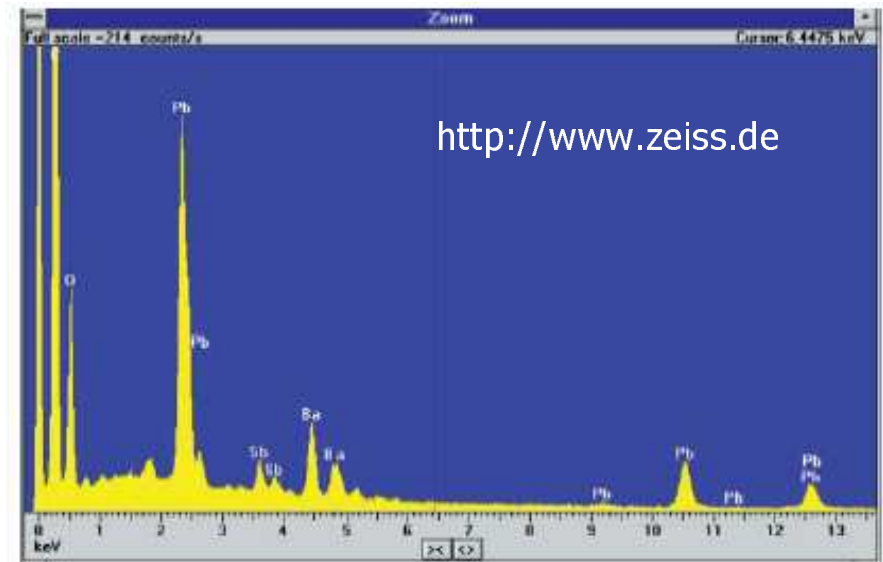
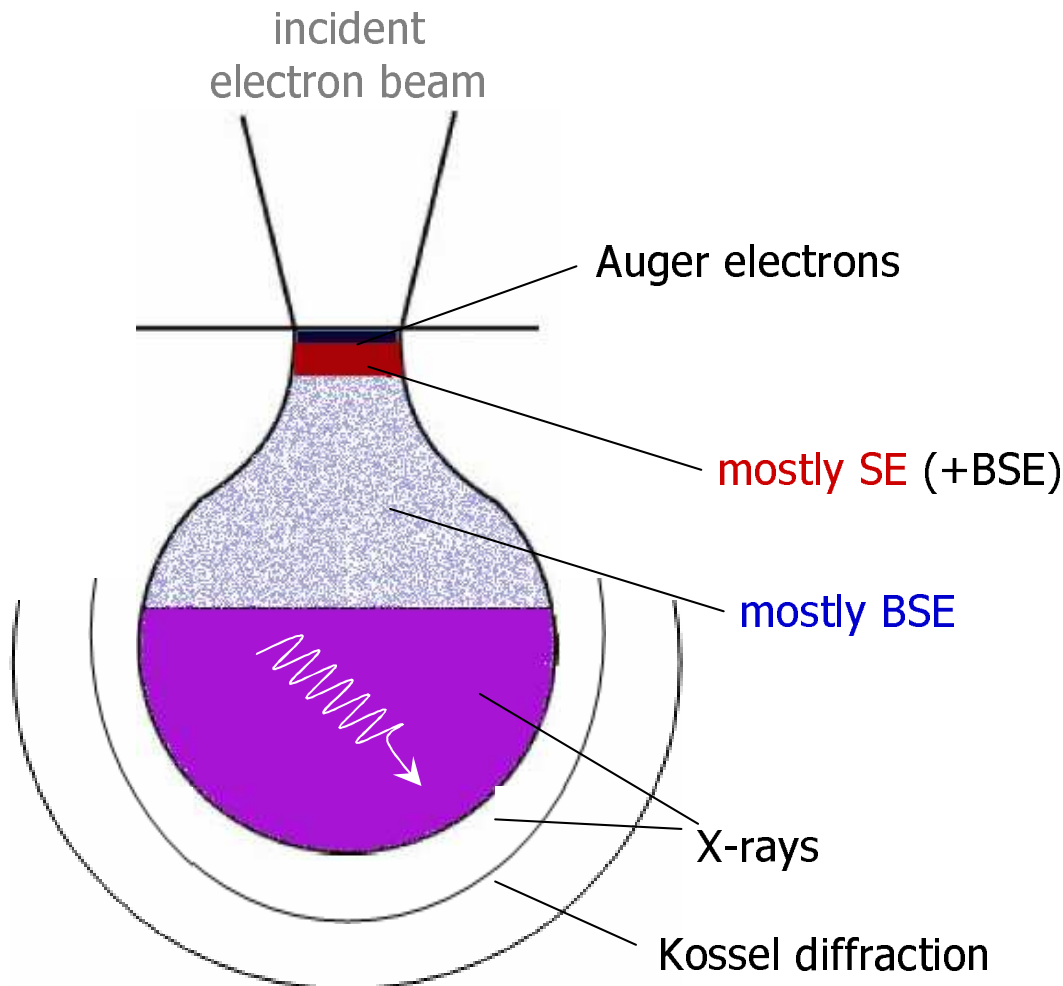
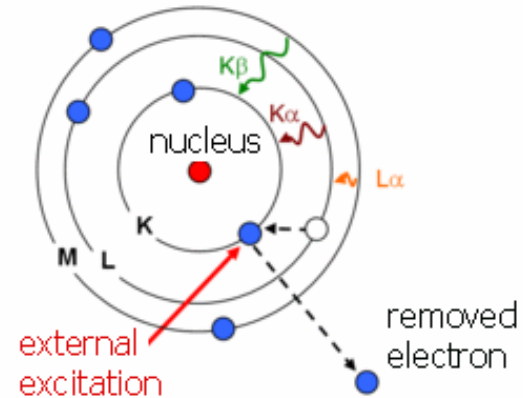
Some atomic contrast:
BSE produce SE \Rightarrow heavier elements
tend to produce more SE

Compositional contrast

The higher the atomic number z ,
the brighter is the contrast

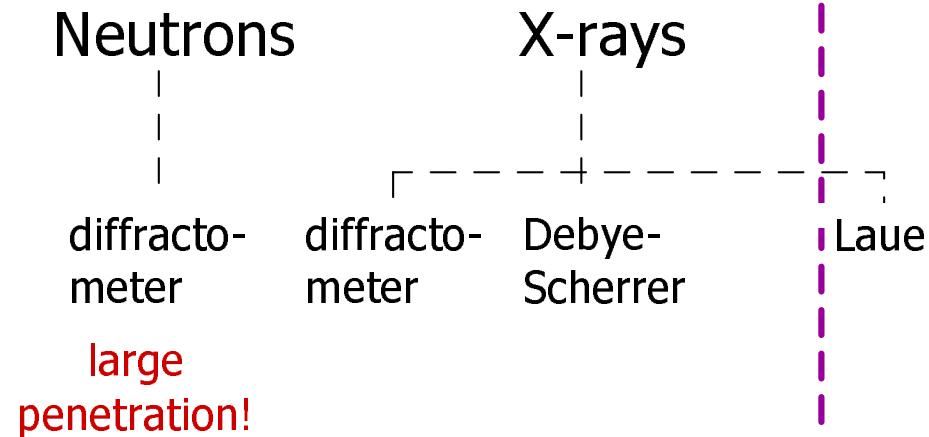
Energy dispersive x-ray spectroscopy (EDX)

EDX → element characteristic x-rays produced during discrete energy lowering of high shell e^- into free states created by inelastic interaction of incident beam with low shell e^-



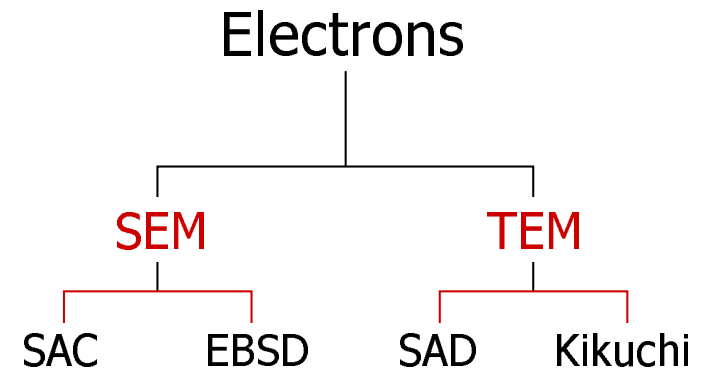
Spectrum from detected particle showing presence of Pb, Ba and Sb

Macrotecture



Def.: volume fraction of the sample having a particular orientation (obtained from the intensity of diffraction from certain planes)

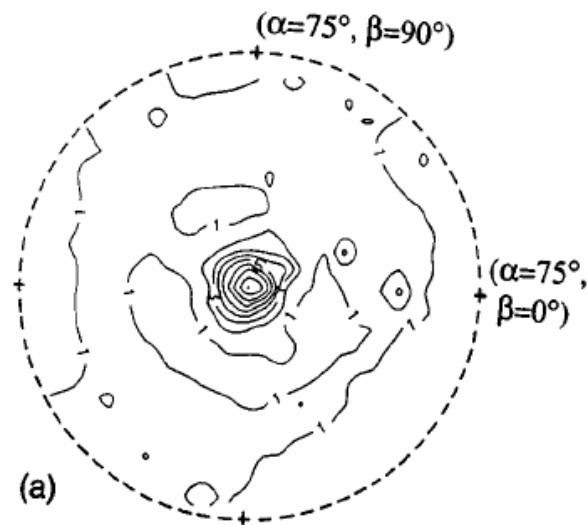
Microtexture



local orientation of individual grains and their spatial location

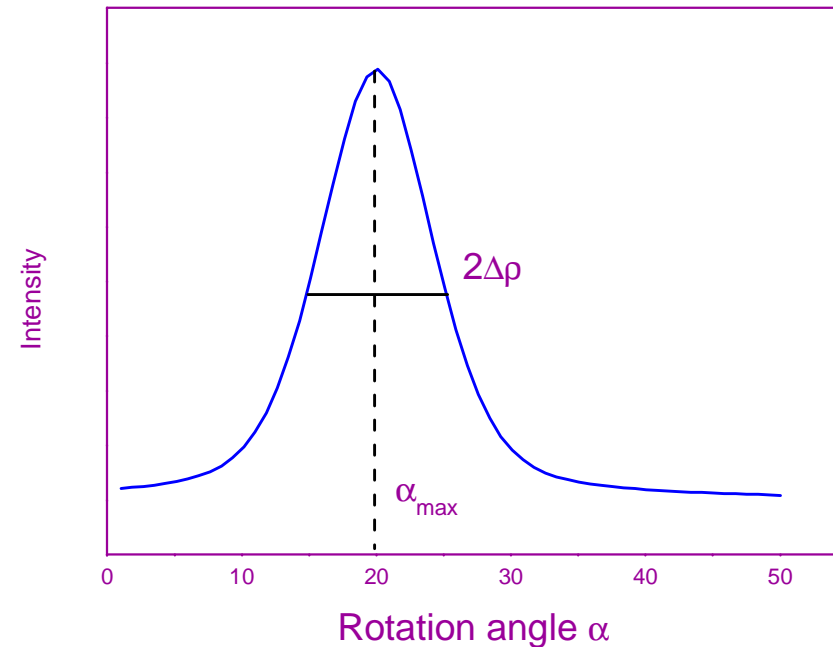
Usual way → pole figure measurements (the statistical directional distribution of poles to a specific lattice plane in a polycrystalline aggregate).

(006) pole figure
for deformed die-upset Nd-Fe-B



Y.R. Wang et al., JAP 81 (1997)

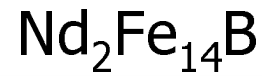
deformation
direction



A detector is positioned on the centre of a diffraction peak hkl and the sample is rotated
 $I_{hkl} \sim$ number of lattice planes

Problems:

- time consuming (need several reflections for ODF construction)
- complicated in case of low symmetry, peak overlap



Isotropic

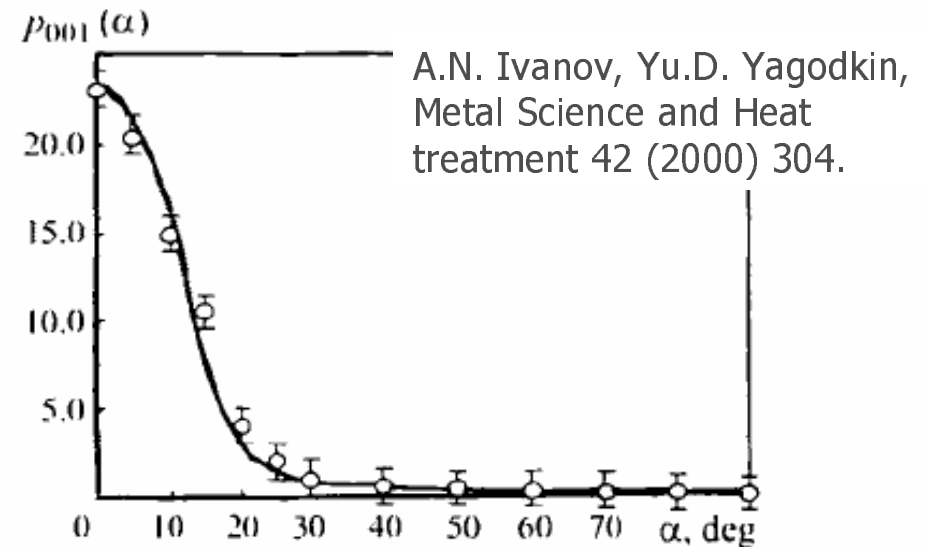
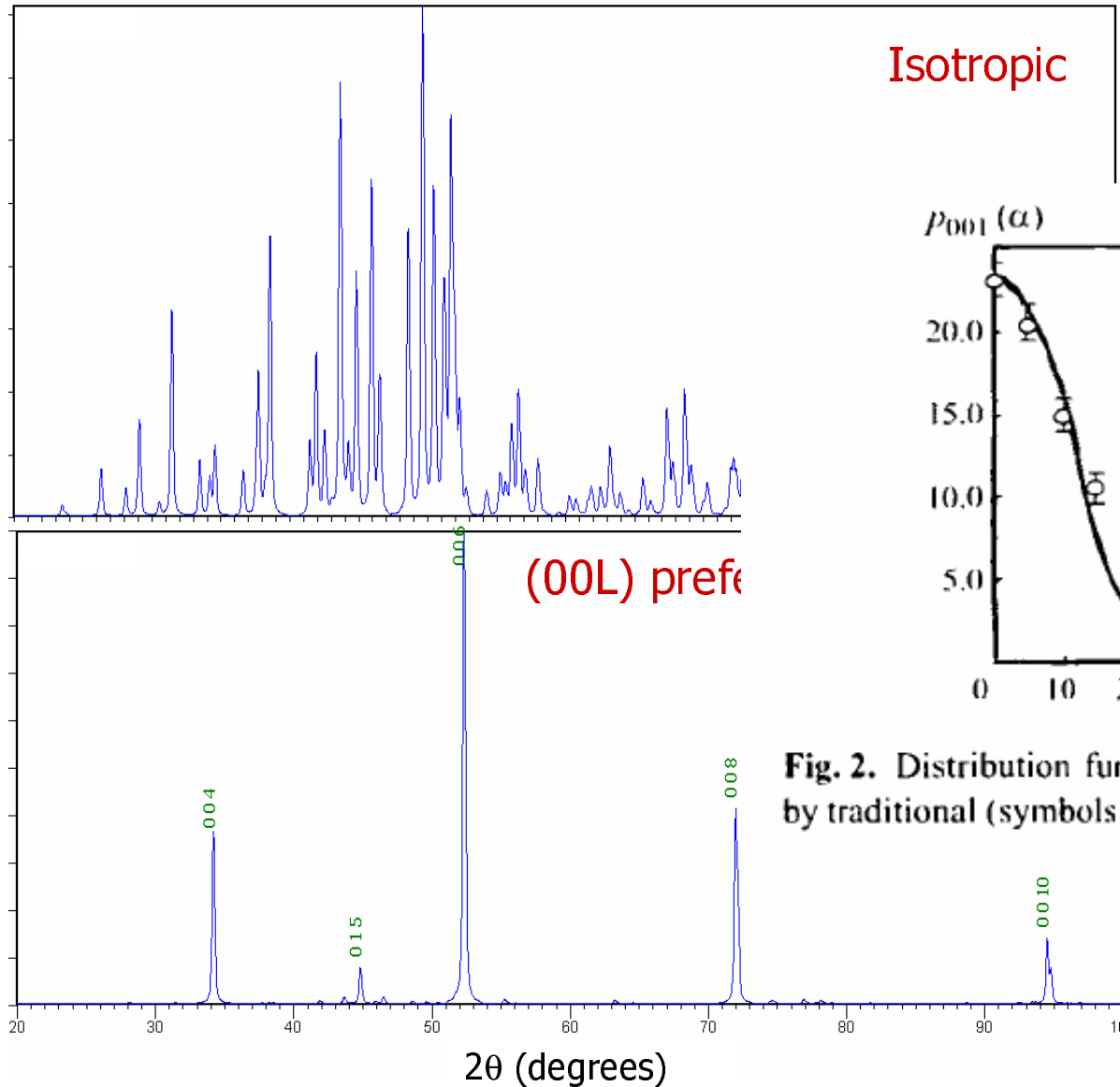


Fig. 2. Distribution function of the pole density $p_{001}(\alpha)$ obtained by traditional (symbols) and rapid (solid line) methods.

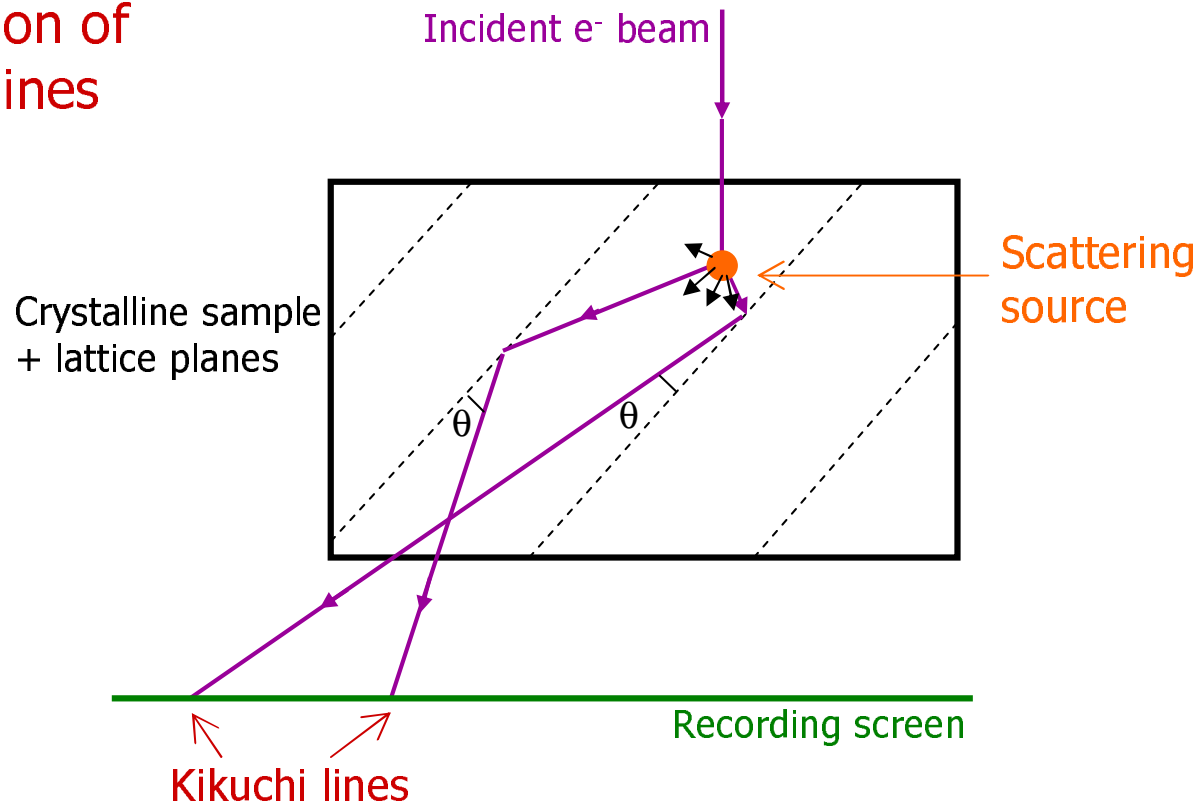
Microtexture → orientation statistics of individual grains and their spatial location

Inelastic scattering
of incident e^-



Elastic scattering
 $2d_{hkl} \sin\theta = n\lambda$

Generation of Kikuchi-lines 2D



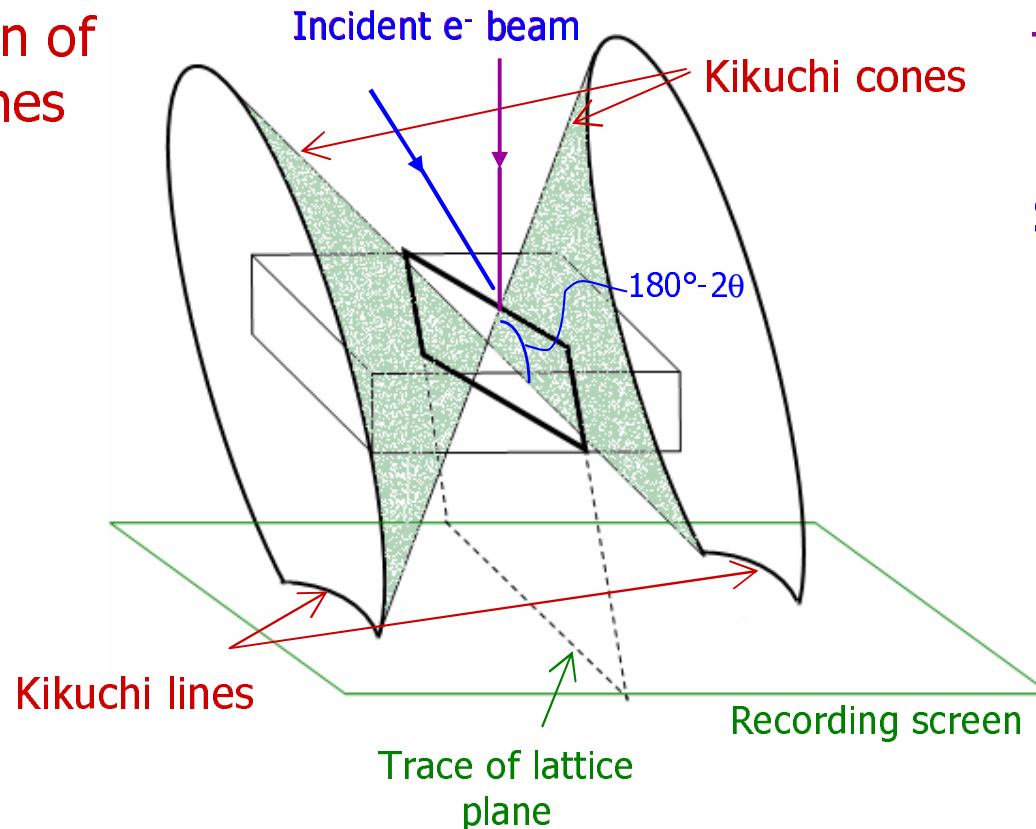
Microtexture → orientation statistics of individual grains and their spatial location

Inelastic scattering
of incident e^-



Elastic scattering
 $2d_{hkl} \sin\theta = n\lambda$

Generation of
Kikuchi-lines
3D



TEM:
incident beam \perp surface

SEM: sample tilted

(large samples \Rightarrow absorption)

For electrons $\theta \approx 0.5^\circ \Rightarrow$
cone apex angle $\approx 180^\circ \Rightarrow$
conic sections are almost flat

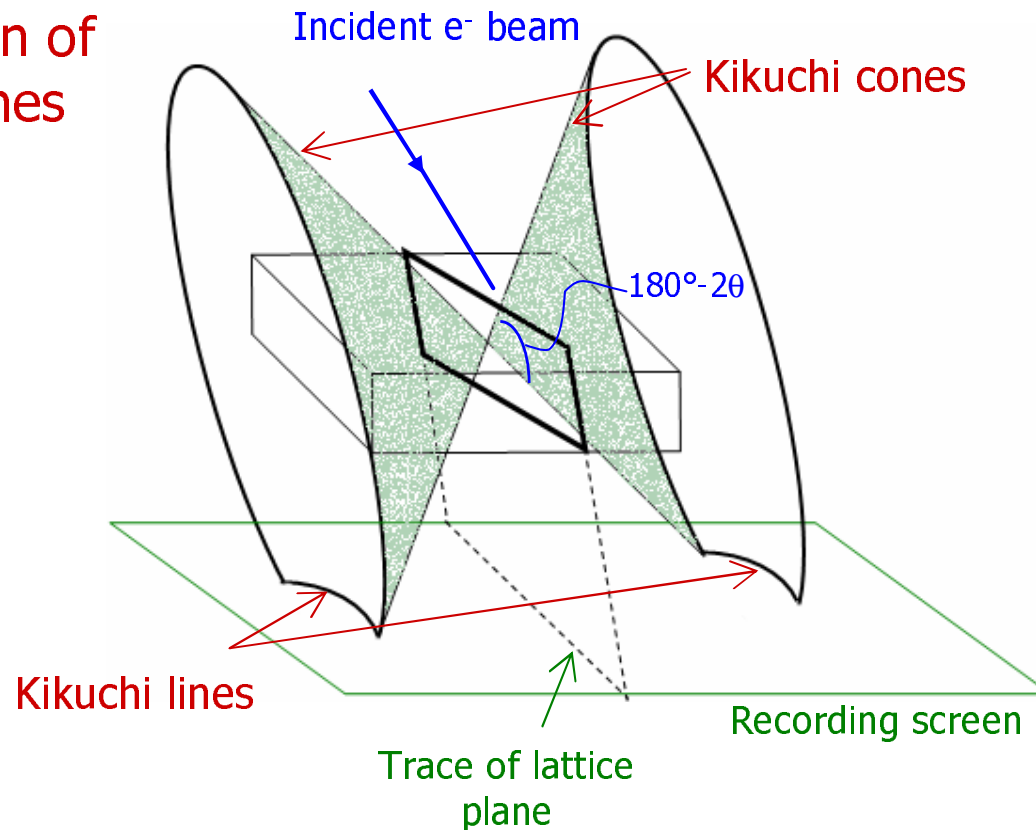
Microtexture → orientation statistics of individual grains and their spatial location

Inelastic scattering
of incident e^-

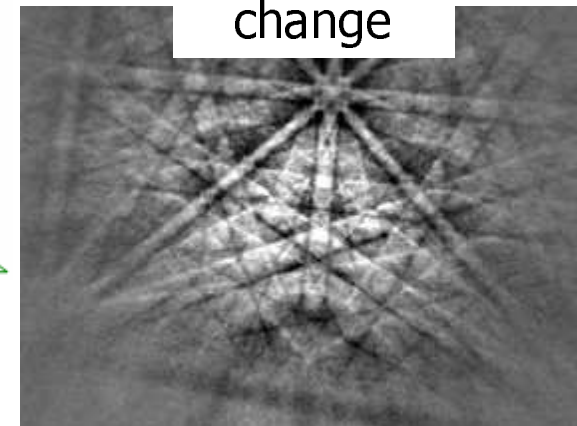
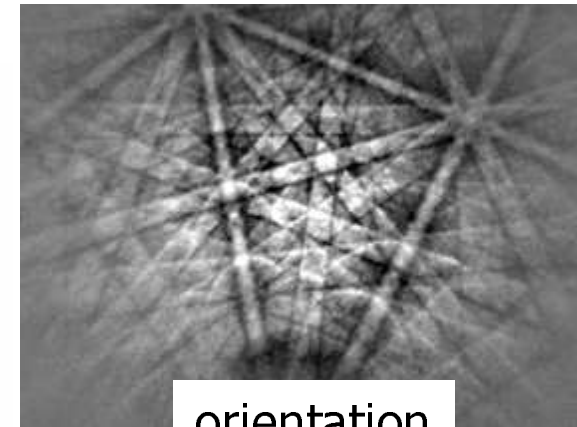


Elastic scattering
 $2d_{hkl} \sin\theta = n\lambda$

Generation of
Kikuchi-lines
3D

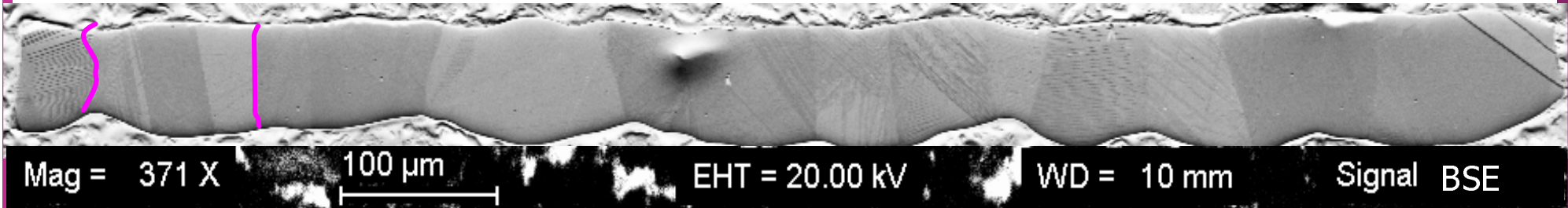


Electron backscattered
diffraction (EBSD) pattern



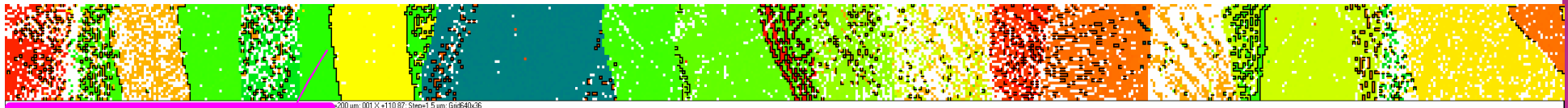
Grain orientation (microtexture) by EBSD

BSE image (tilted sample → topographical contrast)



EBSD orientation map

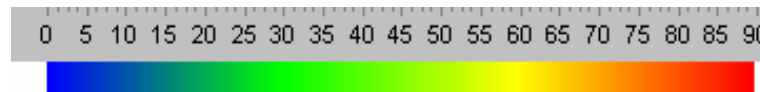
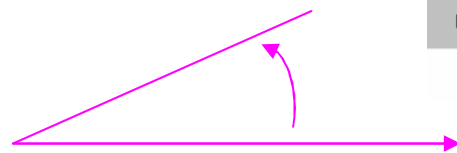
(001) = c-axis (Structure: tetragonal $L2_1$)



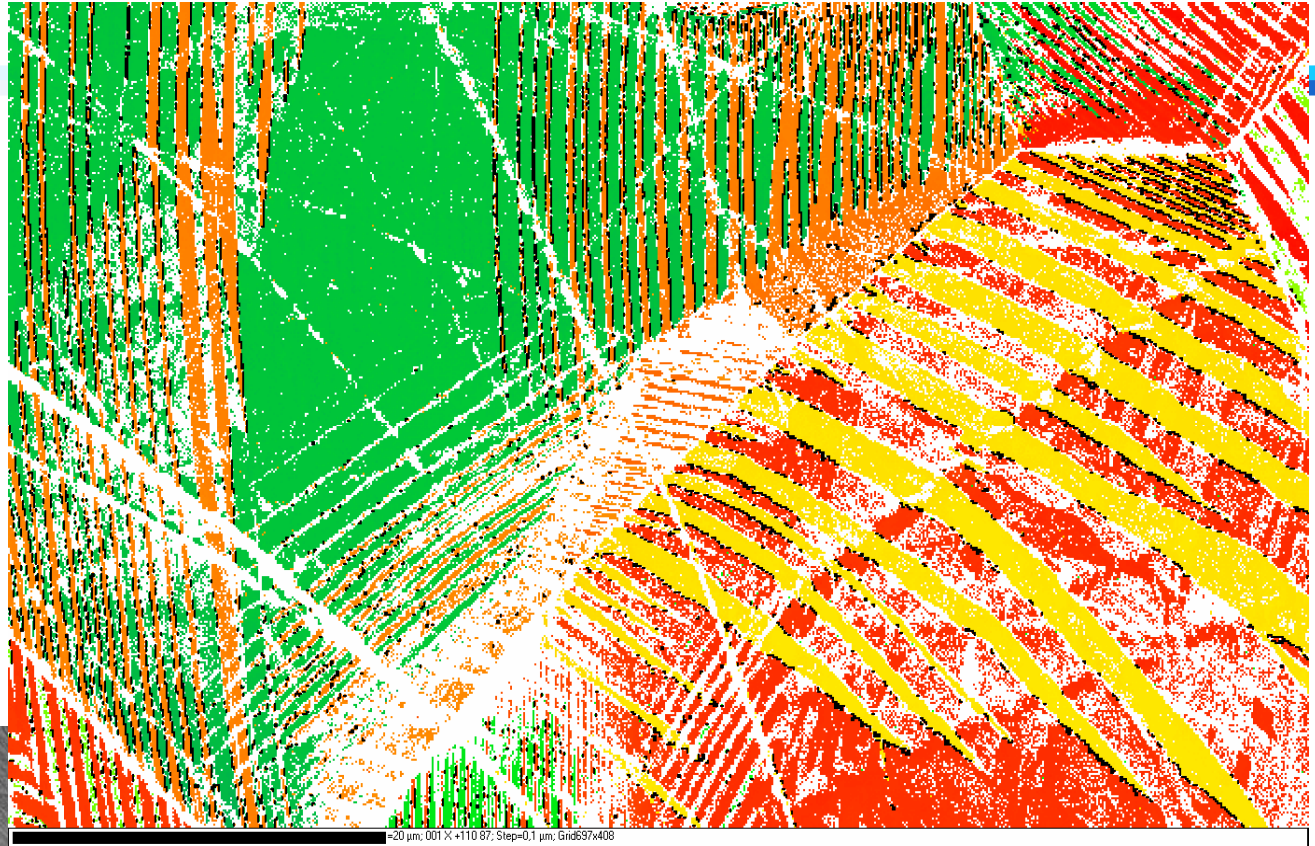
200 μm

Resolution: 1 μm

Black lines – twin boundaries: (110) 87°



Courtesy of N. Scheerbaum



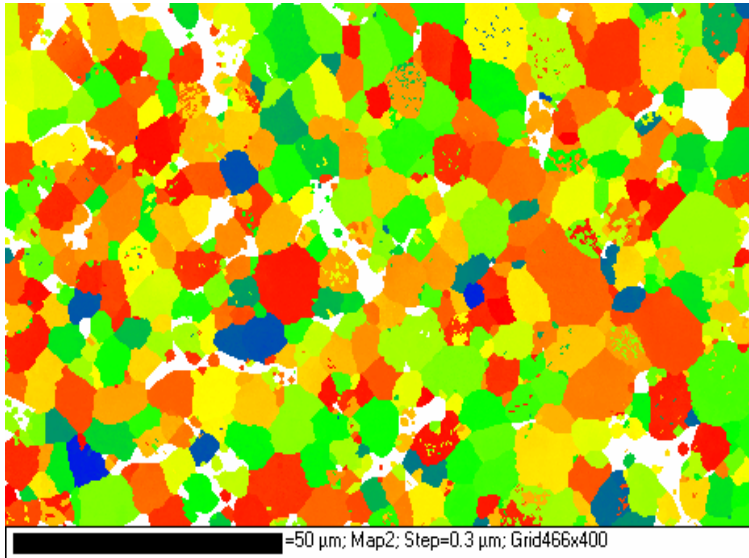
Courtesy of N. Scheerbaum



Black lines: $(110) 87^\circ$

Resolution: $1 \mu\text{m}$

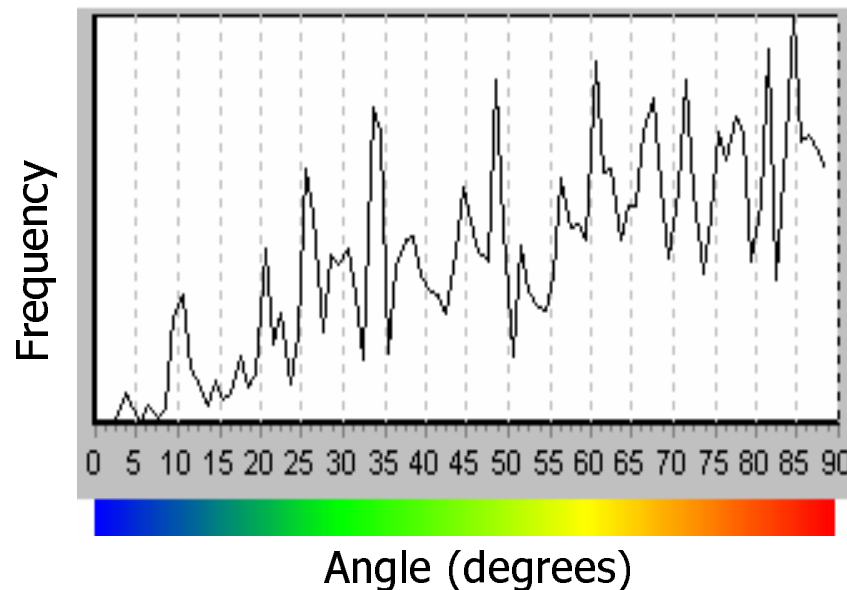
Texture analysis: EBSD



Orientation map from the surface of an isotropic Nd-Fe-B magnet

Resolution here ≈ 50 nm

Possible resolution **10-20 nm!**

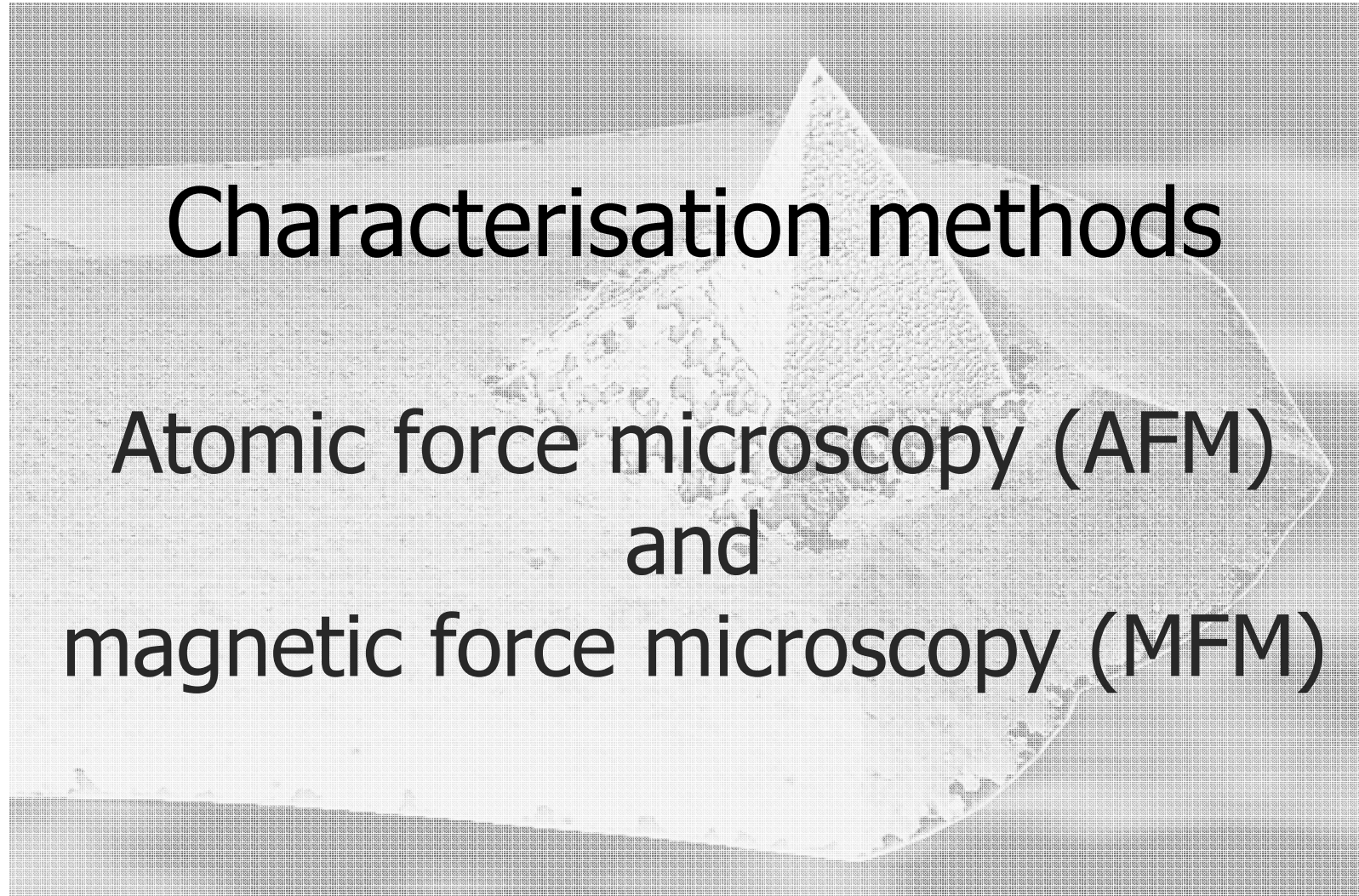


Misorientation angle distribution

(probability of each of the possible grain orientations with respect to the sample coordinates)

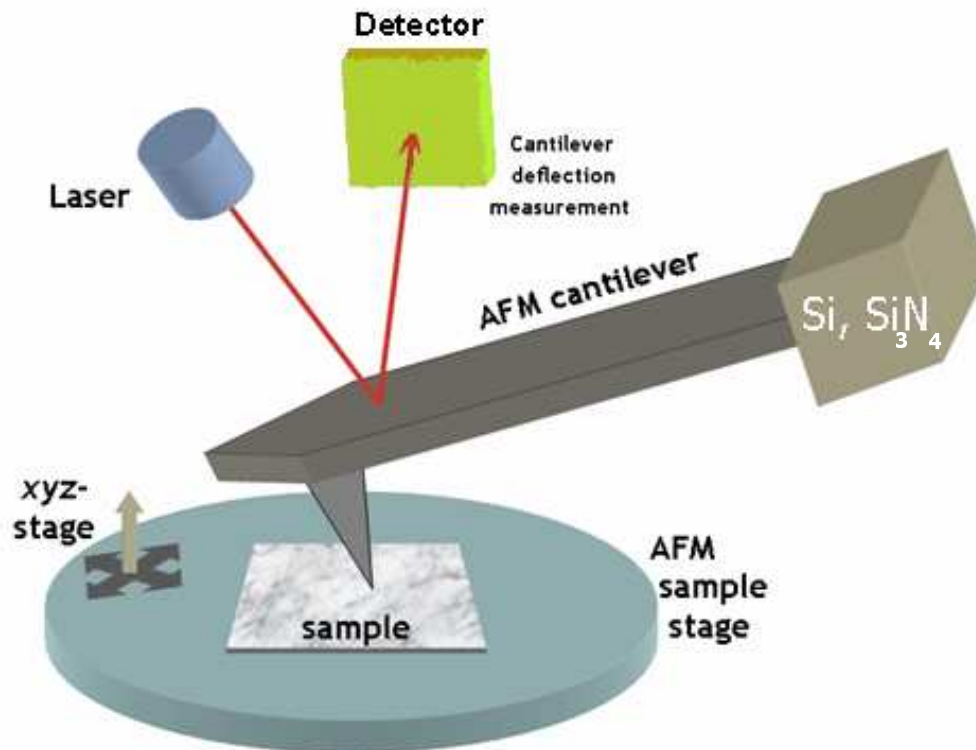
ODF (x-rays/neutrons)

→ averaged over many grains



Characterisation methods

Atomic force microscopy (AFM)
and
magnetic force microscopy (MFM)



Forces measured: mechanical contact, Van der Waals, chemical bonding, electrostatic, magnetic...

Operation modes:

Static (contact and non-contact)

Cantilever is continuously contacting (surface damage) or is held above the sample surface (low resolution)

Dynamic (low amplitude and tapping)

the cantilever is oscillated close to its resonance frequency; amplitude, phase and resonance frequency is modified by tip-sample interaction

Advantages (\Leftrightarrow SEM)

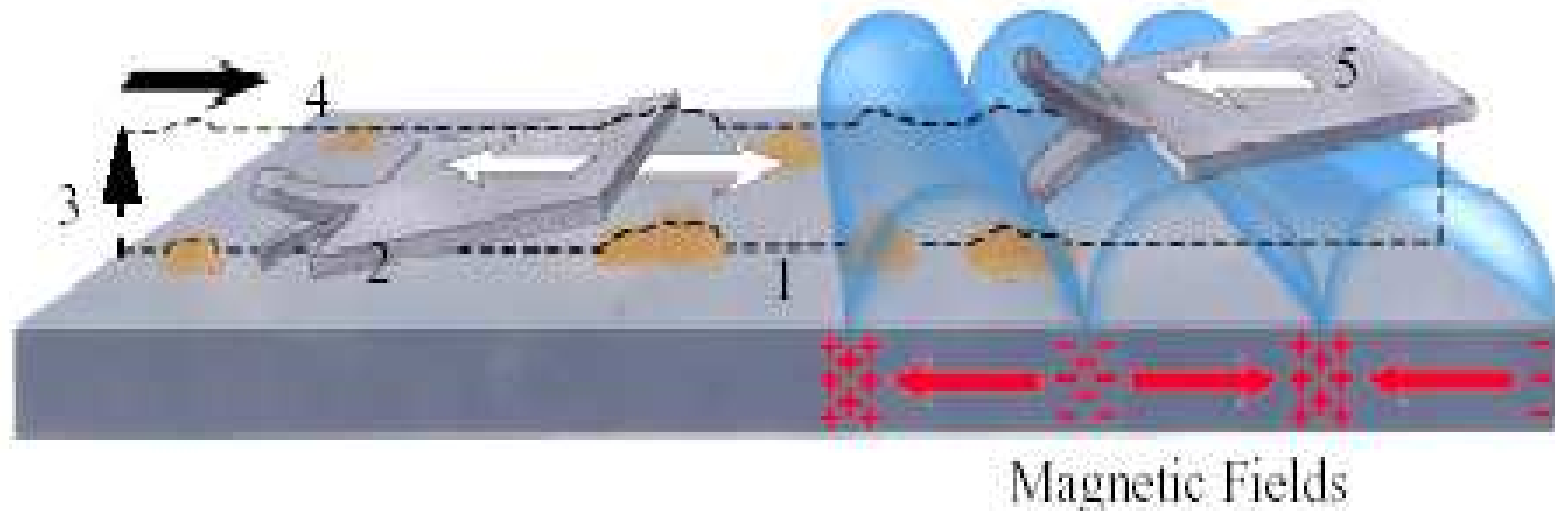
- true 3D surface profile
- non-conducting samples
- can work under ambient conditions (biology etc.)
- atomic resolution under UHV

Disadvantages (\Leftrightarrow SEM)

- maximum scanning area $\sim 150 \times 150 \mu\text{m}$
- slow scanning

Tapping/Lift mode → magnetic and topographic data are separated by scanning twice for each scan line

Lift mode principle



1st scan **tapping mode AFM** (sample topography)

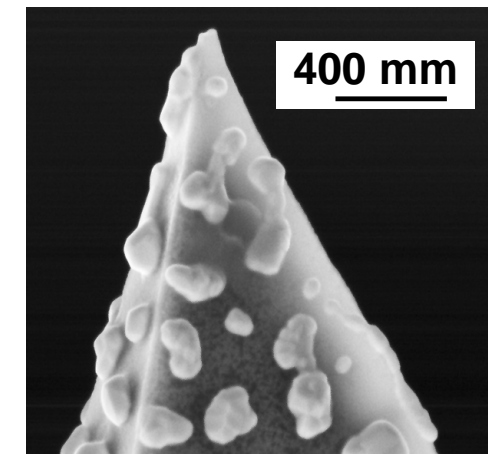
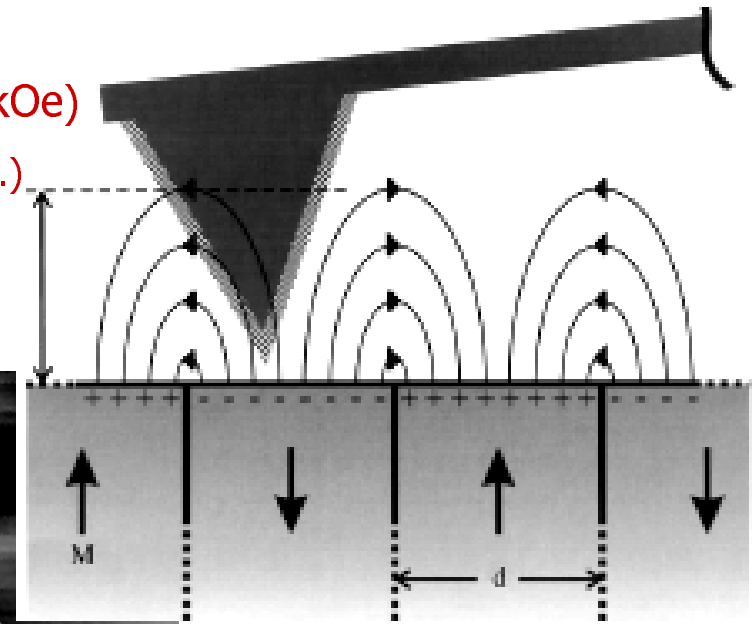
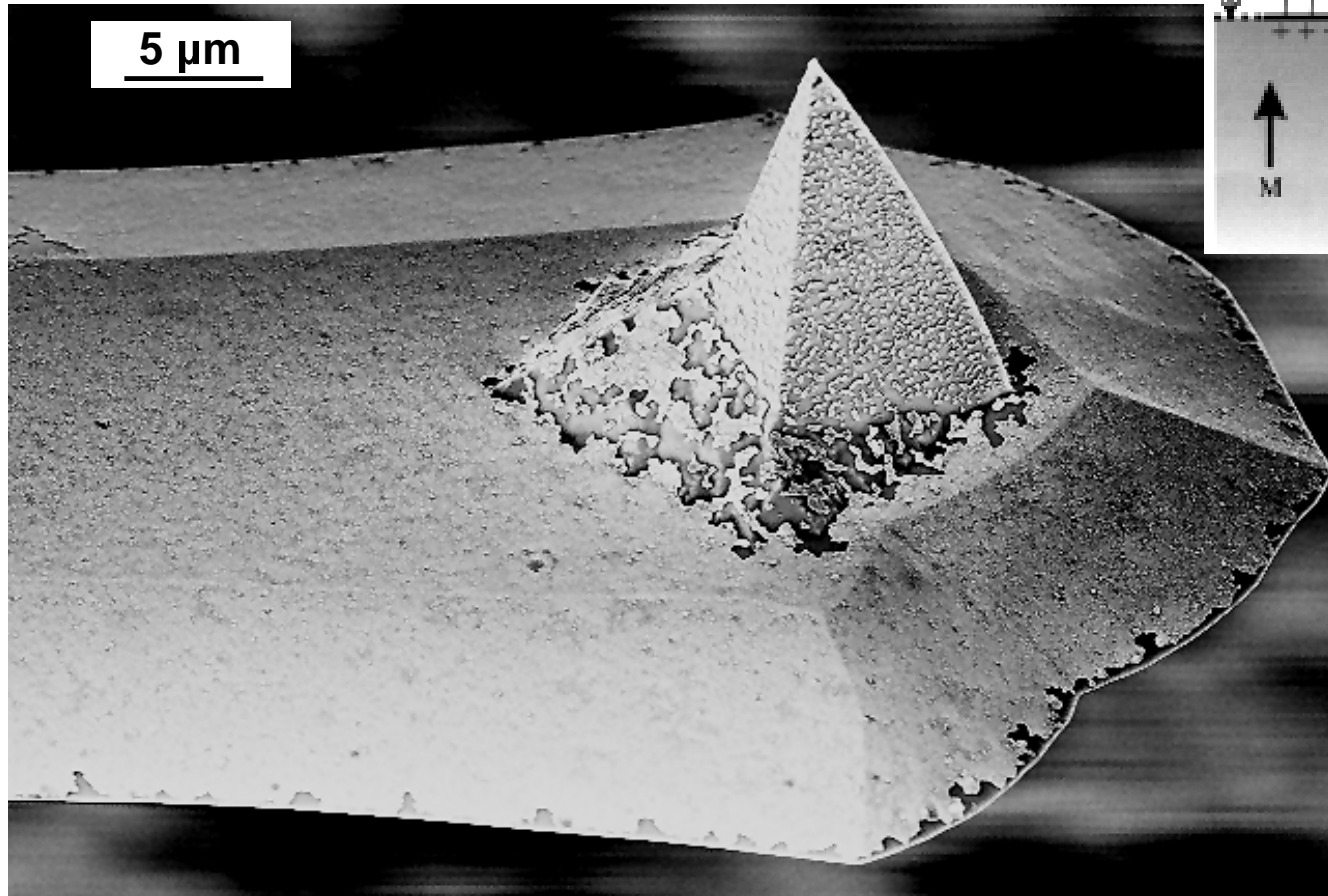
→ close to the sample surface with a constant amplitude of 5-50 nm;
bump/*depression*: less/*more* room to oscillate – amplitude decreases/increases

2nd scan **lift mode MFM** (magnetic force gradient)

→ follows the recorded topography, but at an increased scan height to avoid the van der Waals forces that provided the topographic data

Imaging high anisotropy materials

- high coercivity tips are required (e.g. CoCr coating $H_c \approx 4$ kOe)
- for high resolution (limited to ≈ 50 nm due to dipole-dipole inter.)
 - small tip radius
 - lift height: 100 nm (restricted by large magn. forces)

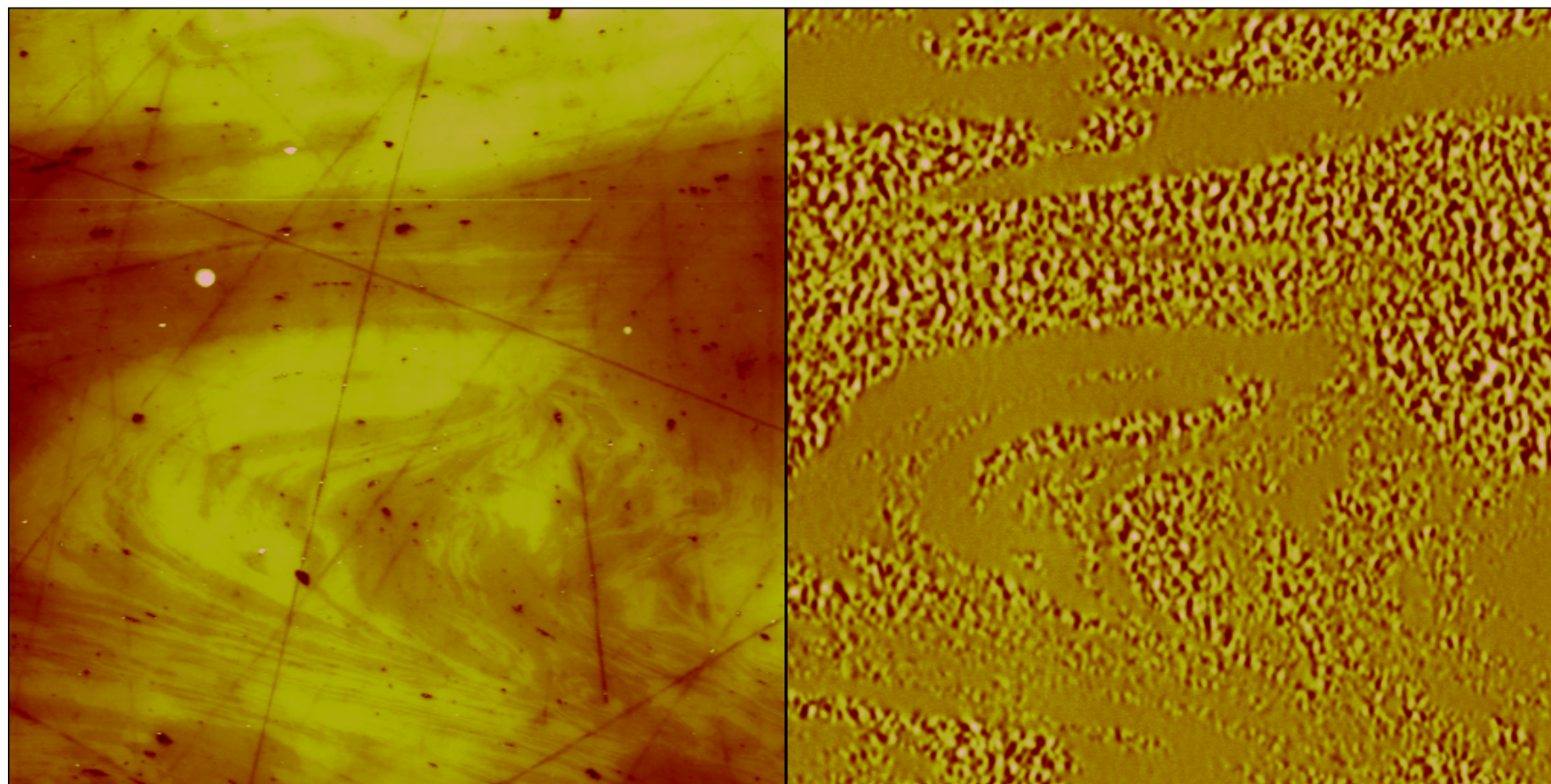


nominal tip radius
of curvature: 40-65 nm

Nanocomposite $L1_0$ FePt / $L1_2$ FePt₃

Tapping mode AFM

Lift mode MFM



0 30.0 μm 0

Data type
Z range

Height
100.0 nm

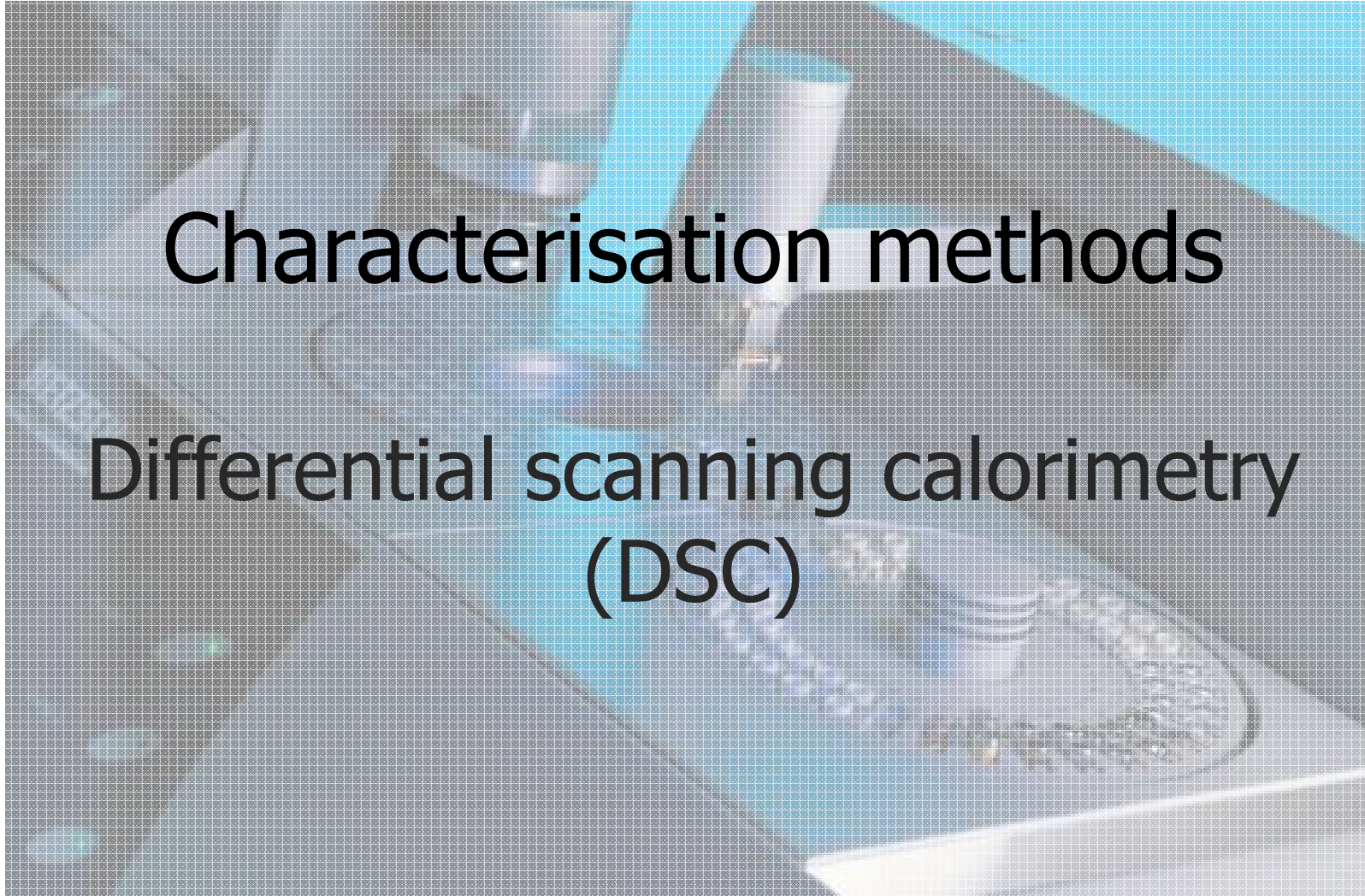
Data type
Z range

Phase
15.00 $^{\circ}$

0 30.0 μm

Characterisation methods

Differential scanning calorimetry (DSC)



Thermal analysis: definitions

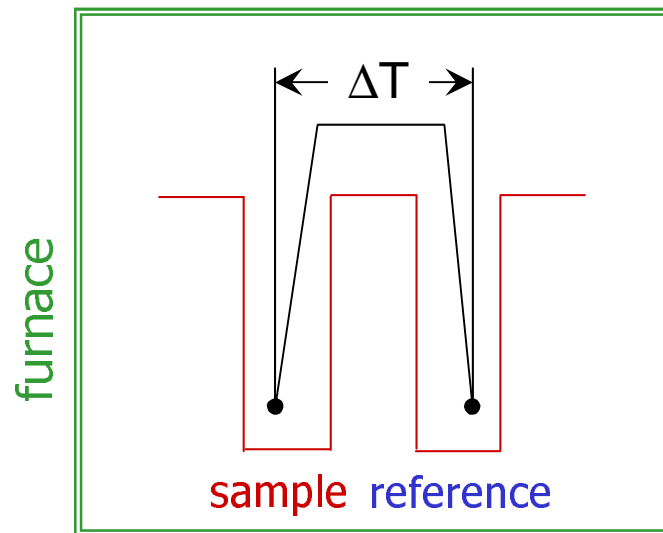
Differential thermal analysis (DTA) → the temperature difference between a sample and a reference, ΔT , is measured as both are subjected to identical heat treatments

Calorimeter → measures heat absorbed or evolved during heating or cooling

Differential calorimeter → measures heat ... relative to a reference

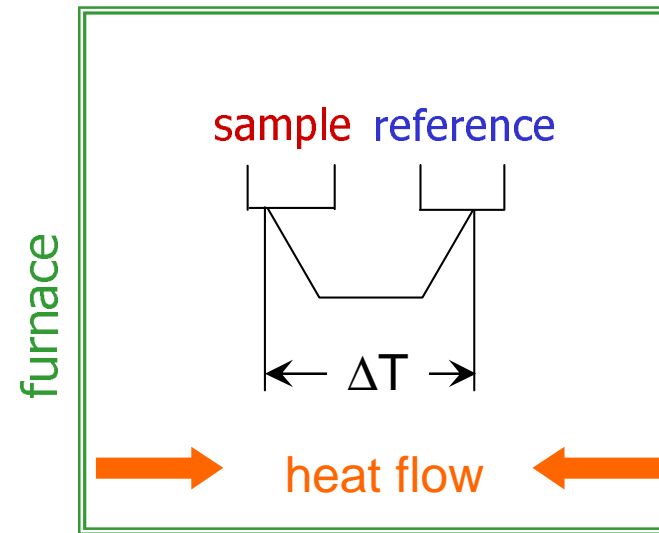
Differential scanning calorimeter (DSC) → does the above + ramps the temp. up or down

DTA



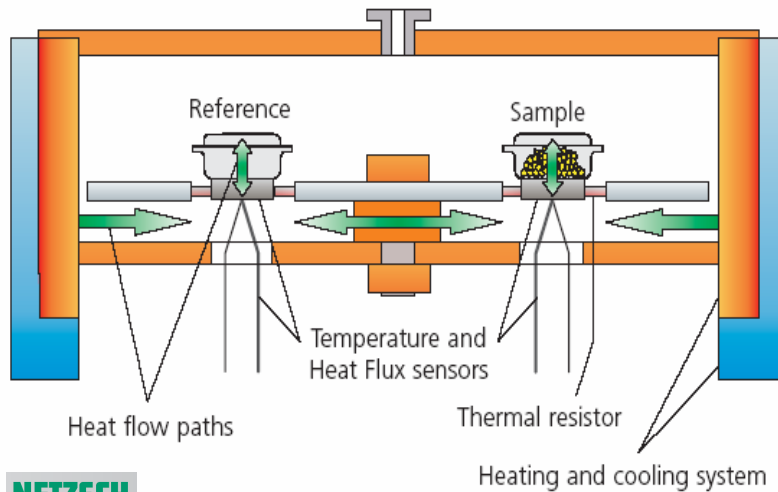
$$\Delta T = T_S - T_R$$

"Calorimetric" DTA or heat-flux DSC



The sample and the reference are maintained at the **same temp.!**

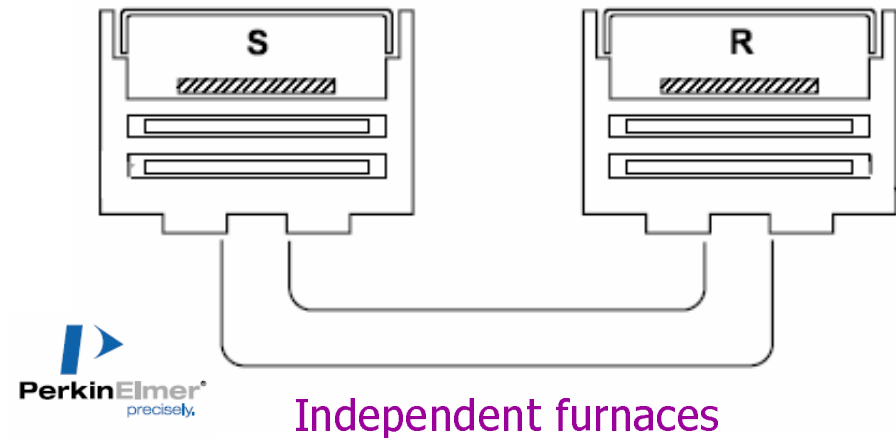
Heat-flux DSC




Basis: a homogeneous temperature field in the furnace

⇒ temperature gradients at the thermal resistances of the sensor

Power-compensated DSC



Basis: the system is maintained at a "thermal null" state at all times

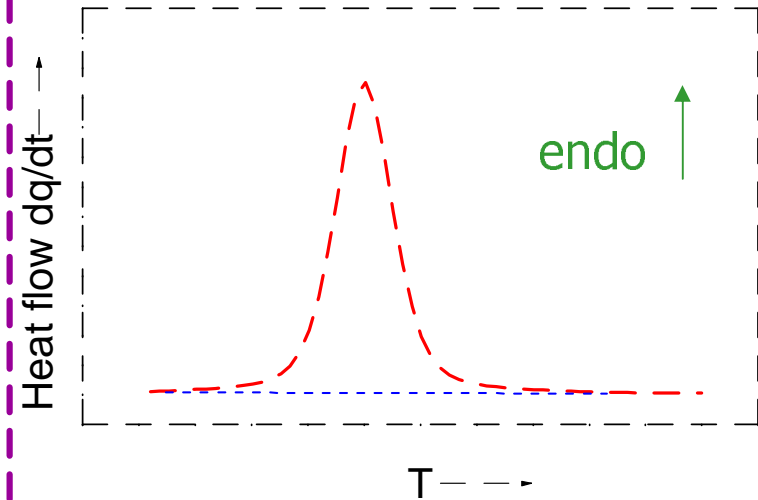
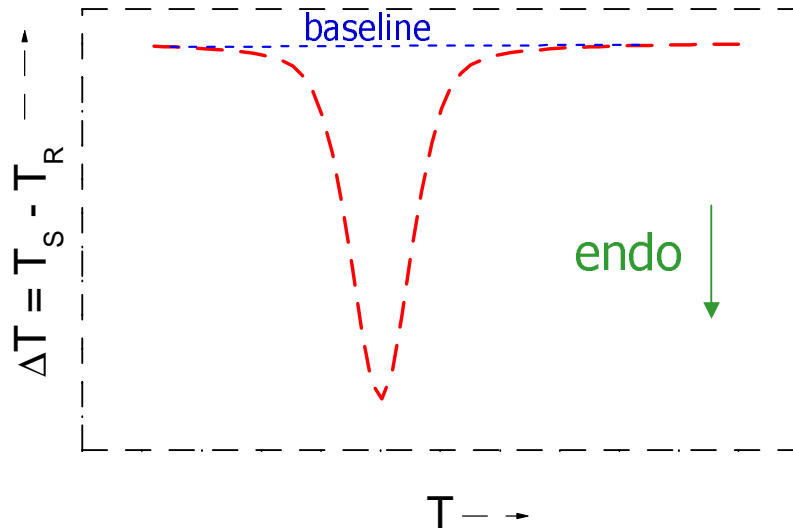
⇒ power (energy) is applied to or removed from the calorimeter to compensate for the sample energy

Heat absorption or loss due to a transition in the sample,
difference in c_p between the reference and sample

DTA

Heat-flux DSC

Power-compensated DSC



$$T_{SM} = T_S \quad T_{RM} = T_R$$

$$T_{heater} \neq T_{SM} \neq T_S$$

$$\Delta T = T_R - T_S = R(dT/dt)(C_p^S - C_p^R)$$

$$\Delta T = T_{RM} - T_{SM} = R(dT/dt)(C_p^S - C_p^R)$$

R – thermal resistance. Difficult to calculate!

$$R = f(\text{instrument}, S, R)$$

$$R = f(\text{instrument})$$

$$\text{Flux equation: } dq/dt = (1/R)\Delta T$$

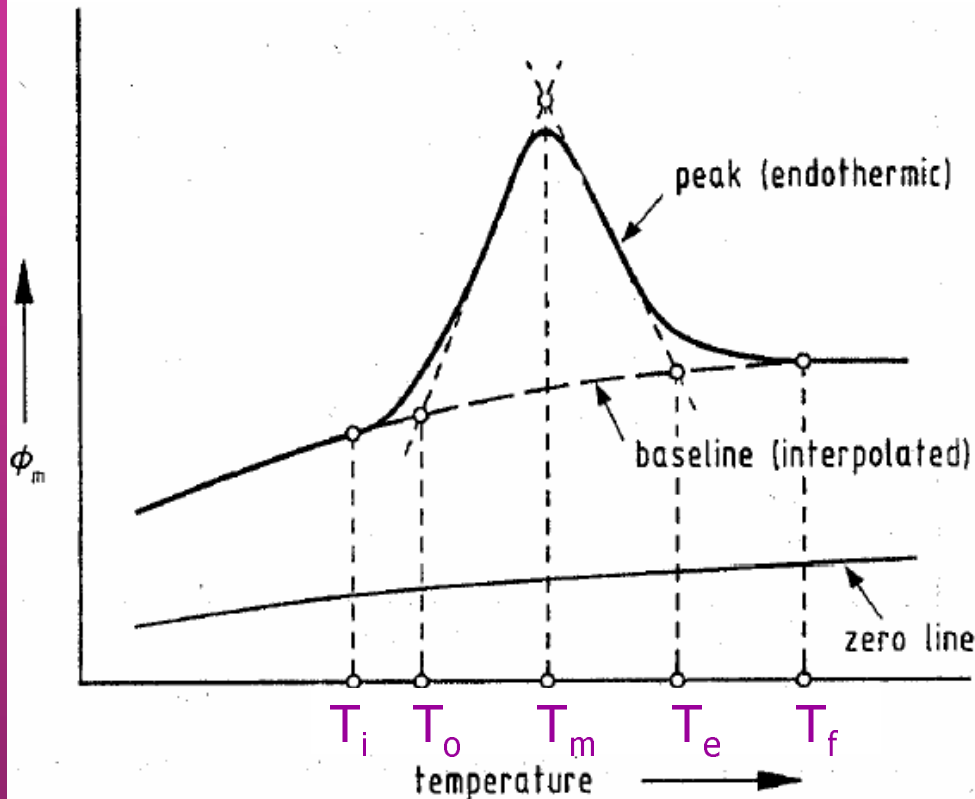
Power is varied to make $T_{SM} = T_{RM}$

$$R = 0!$$

Power \sim energy changes in a sample. Signal is measured directly!

$$\Delta(dq/dt) = (dT/dt)(C_p^S - C_p^R)$$

Characteristics of a DSC curve



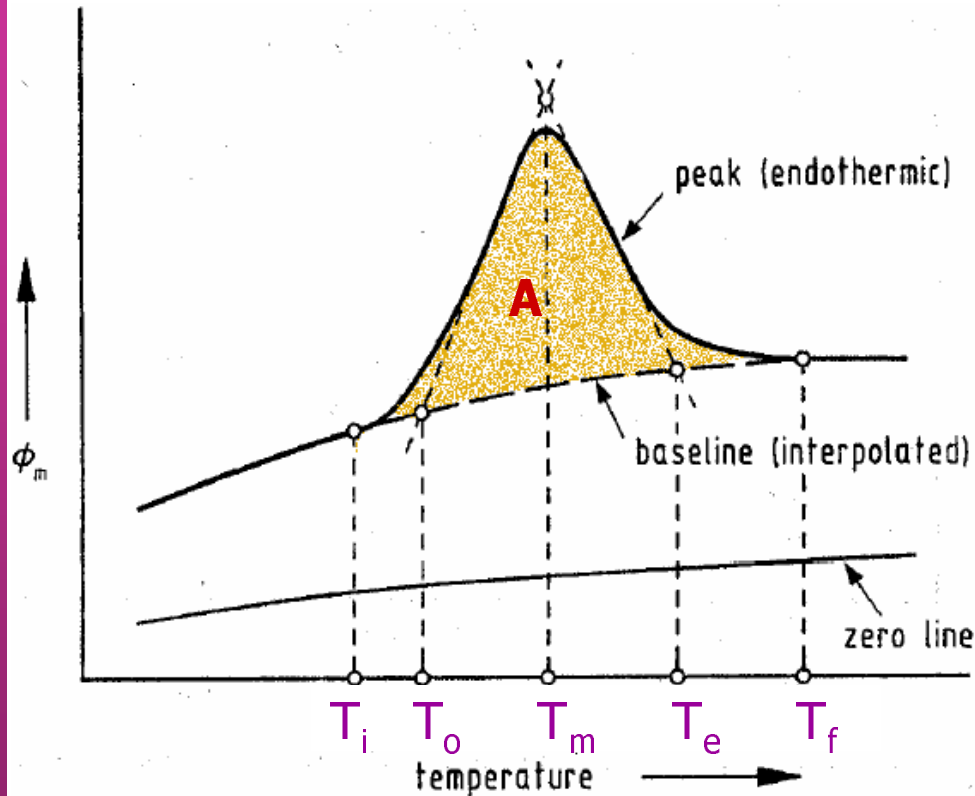
Zero line: empty instrument or empty crucibles

Baseline: connects the curve before and after the peak

Peak temperatures:

initial T_i ; onset T_o ; peak maximum T_m ; completion T_e ; final T_f

Characteristics of a DSC curve



Zero line: empty instrument or empty crucibles

Baseline: connects the curve before and after the peak

Peak temperatures:

initial T_i ; onset T_o ; peak maximum T_m ; completion T_e ; final T_f

Enthalpy change: $\Delta H = A \times K/m$

A – area, **m** – sample mass, **K** – calibration factor ($A \Leftrightarrow \Delta H$ by melting of a pure metal)

Heat capacity c_p : $\Delta H = \int_{T_1}^{T_2} c_p dT$

What can be measured in DSC?

Exothermic events

crystallisation

solid-solid transitions

decomposition

ordering

chemical reactions

Endothermic events

melting

sublimation

solid-solid transitions

disordering

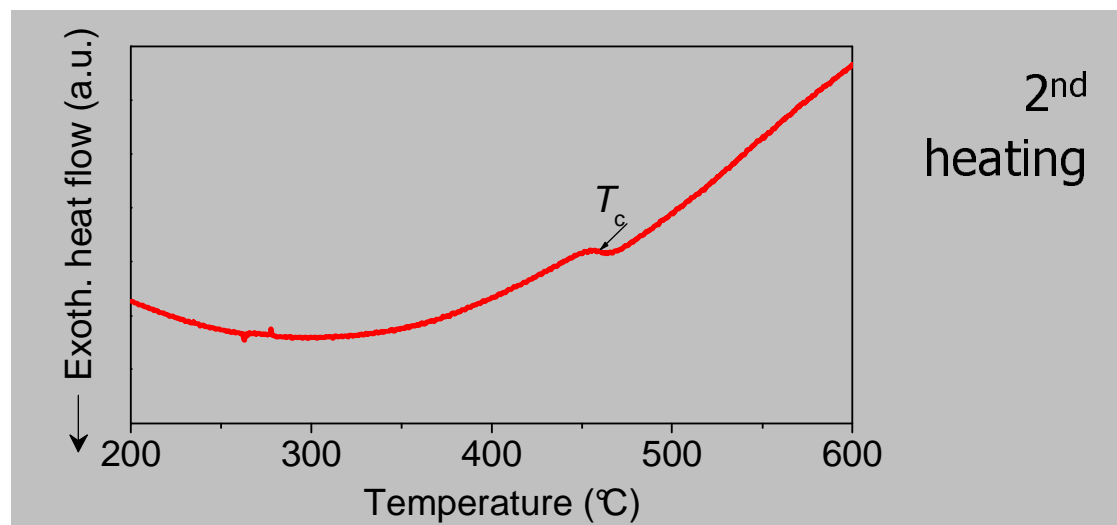
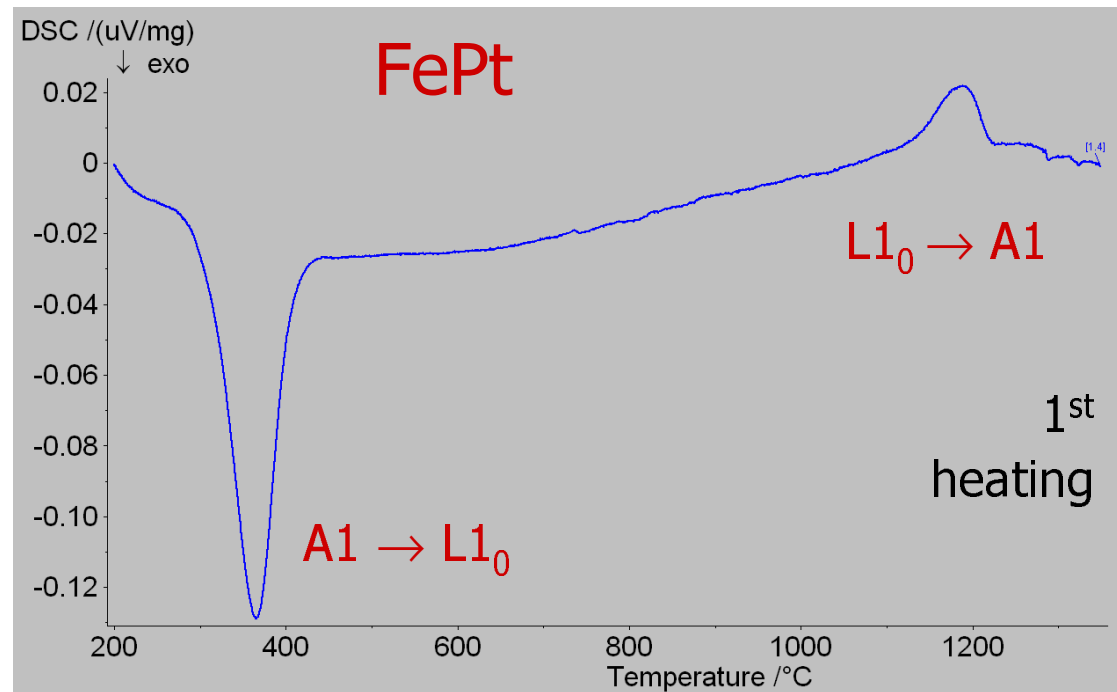
chemical reactions

2nd order-type transitions

(c_p change)

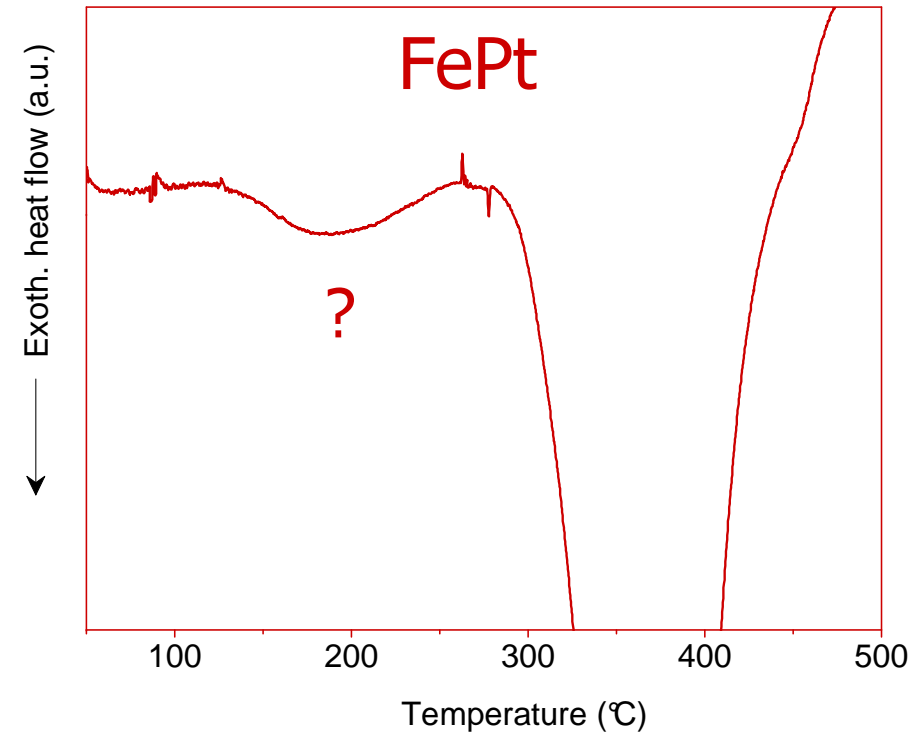
glass transition

Curie point



What can be measured in DSC?

Exothermic signal → healing out of crystal defects



Interpretation of DSC data → use of additional techniques!

XRD, microscopy, spectroscopy...

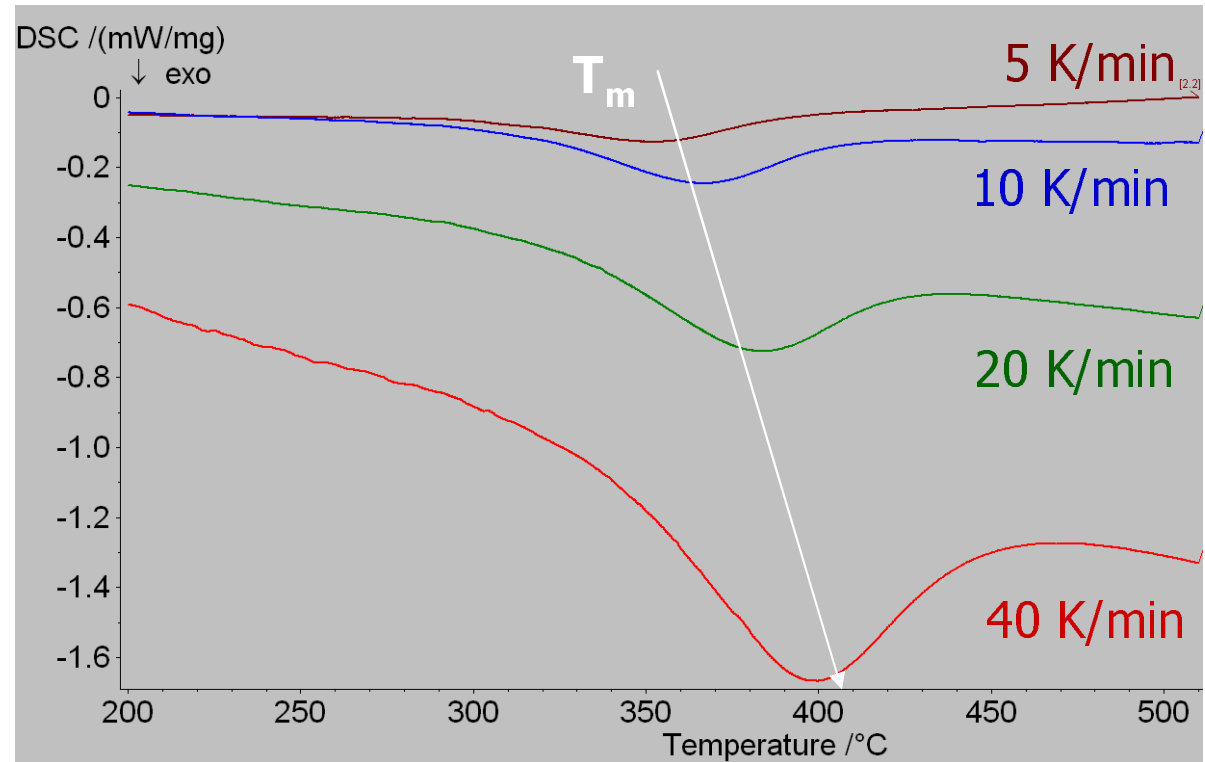
Kinetically controlled transitions
(diffusion, crystallisation,
ordering etc.)

shift to higher temp. with
increasing heating rate

The total heat flow increases
linearly with heating rate due
to c_p of the sample

↑ heating rate ↑ sensitivity;
↓ heating rate ↑ resolution

For obtaining values close to
true thermodynamic slow
heating rates (1-5 K/min)
should be used



Isothermal mode

$$d\alpha / dt = A \exp(-E_a / k_B T) f(\alpha)$$

Temperature $T = \text{const}$

Procedure:

- measure transformed fraction $\alpha(t)$
- plot $d\alpha/dt = f(t \text{ or } \alpha)$
- determine linearity of $(d\alpha/dt)$ vs. $f(\alpha)$

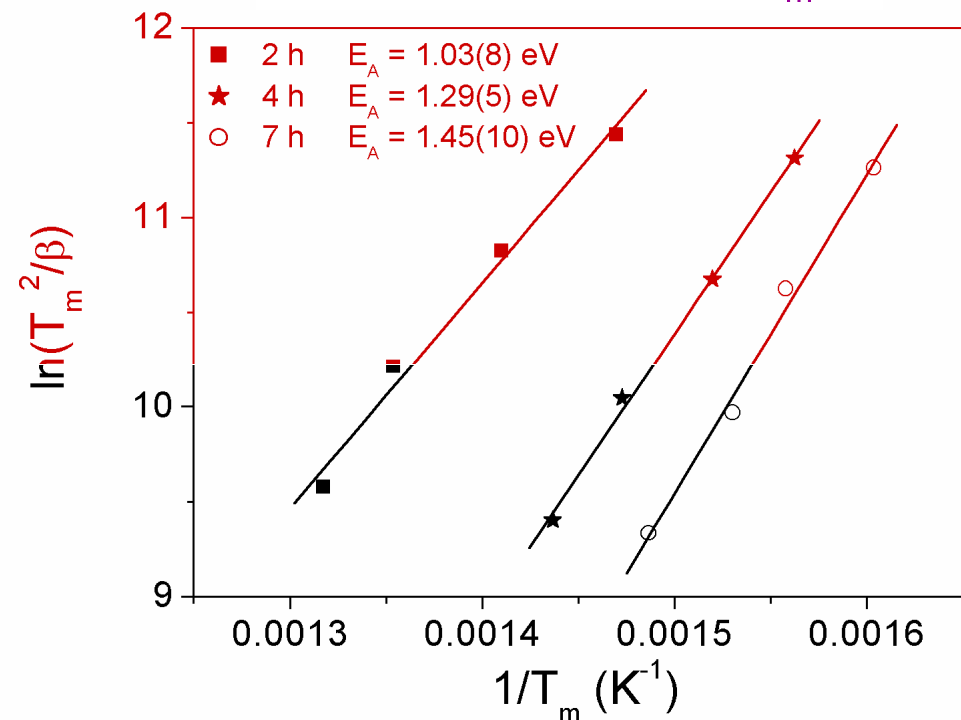
$f(\alpha)$ - conversion function used for the interpretation of reaction mechanism (KJMA kinetics etc.)

- $d\alpha/dt = K f(\alpha) \rightarrow K$ used in Arrhenius plot to calculate activation energy E_a and Arrhenius parameter A

Dynamic (nonisothermal) mode

$$\ln(T_m^2 / \beta) = E_a / k_B T_m$$

Heating rate $\beta = dT/dt = \text{const}$

Kissinger plot for T_m 

Hyper DSC

- a modification of the power-compensated DSC
- very fast scans up to 500 K/min (helps mimic process conditions)

StepScan DSC

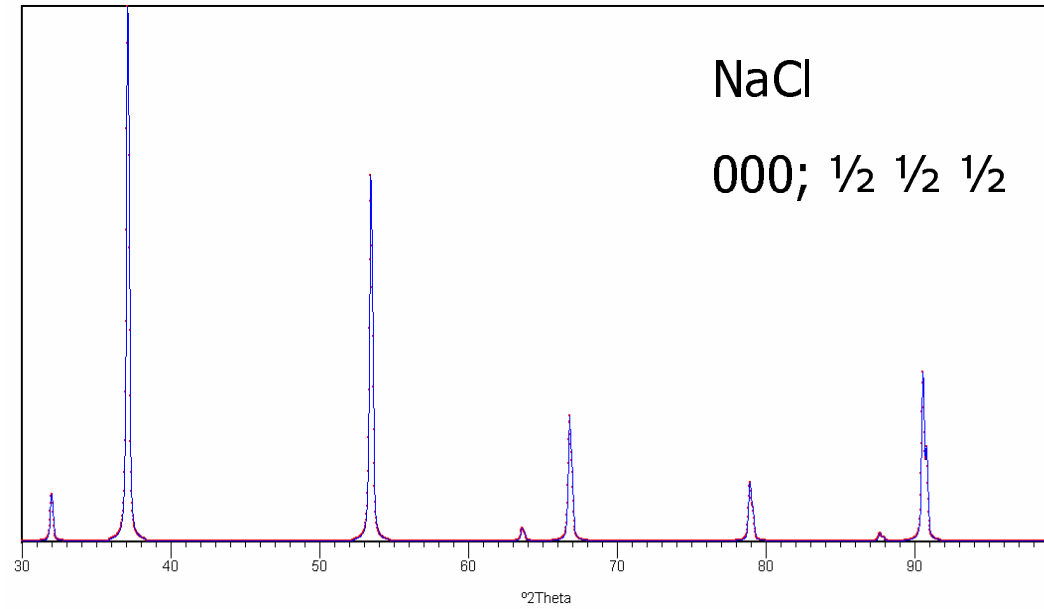
- modulated temperature power-compensated DSC (short interval heating and isothermal-hold steps)
- separates reversible and irreversible effects
- more accurate heat-capacity results since C_p measurements are generated over short-interval temperature segments

$$\text{Total heat flow } dQ/dt = C_p \cdot dT/dt + f(t,T) \longrightarrow \begin{array}{l} \text{non-reversing signal} \\ \text{(kinetic component)} \end{array}$$

$C_p \cdot dT/dt$ reversing signal
heat flow resulting from
temp. modulation (c_p component)

Simultaneous analysis techniques: DSC-TG, DSC-XRD...

Questions?



определить невозможно.

$I_{coh}(Q)$ — интенсивность рассеянного излучения, которую можно измерить экспериментально. Если определить интерференционную функцию $S(Q)$ как

$$S(Q) = I_{coh}(Q)/N b^2, \quad (3.17)$$

то из (3.16) можно получить

$$S(Q) = 1 + \int_0^{\infty} 4\pi r^2 \rho_0 (g(r) - 1) \frac{\sin Qr}{Qr} dr. \quad (3.18)$$

Равенство (3.18) является основной формулой, связывающей измеряемую непосредственно в дифракционных экспериментах интерференционную функцию $S(Q)$ с парной функцией распределения $g(r)$. Функцию $S(Q)$ часто также называют структурным фактором. Реально сначала определяют функцию $S(Q)$, по которой можно затем различным образом найти $g(r)$:

$$g(r) = 1 + \frac{1}{2\pi^2 \rho_0 r} \int_0^{\infty} (S(Q) - 1) Q \sin Qr dr. \quad (3.19)$$

Представим атом, находящийся в некоторой начальной точке, сферой радиусом r , ведя отсчет от ее геометрического центра. Распределение плотности атомов, находящихся на внешней поверхности этой сферы, определяется как функция радиального распределения (ФРР) и равно $4\pi r^2 \rho_0 g(r)$.